SYNTHESIS AND CHARACTERIZATION OF $CaCu_3Ti_4O_{12}$ AND LANTHANUM DOPED $CaCu_3Ti_4O_{12}$ BY AUTO-COMBUSTION TECHNIQUE

A

THESIS SUBMITTED IN THE PARTIAL FULFILLMENT OF THE REQUIREMENT FOR THE DEGREE OF

MASTER OF TECHNOLOGY

IN

CERAMIC ENGINEERING

BY

SUNIL PATRA
Roll No-207CR108

DEPARTMENT OF CERAMIC ENGINEERING
NATIONAL INSTITUTE OF TECHNOLOGY, ROURKELA
2009

SYNTHESIS AND CHARACTERIZATION OF $CaCu_3Ti_4O_{12}$ AND LANTHANUM DOPED $CaCu_3Ti_4O_{12}$ BY AUTO-COMBUSTION TECHNIQUE

A

THESIS SUBMITTED IN THE PARTIAL FULFILLMENT OF THE REQUIREMENT FOR THE DEGREE OF

MASTER OF TECHNOLOGY

IN

CERAMIC ENGINEERING

BY
SUNIL PATRA

UNDER THE GUIDANCE OF

Prof. S. K. PRATIHAR AND Prof. R. MAZUMDER

DEPARTMENT OF CERAMIC ENGINEERING
NATIONAL INSTITUTE OF TECHNOLOGY, ROURKELA
2009

Department of Ceramic Engineering
National Institute of Technology
Rourkela-769008

CERTIFICATE

This is to certify that the thesis on **"SYNTHESIS AND CHARACTERIZATION OF $CaCu_3Ti_4O_{12}$ AND LANTHANUM DOPED $CaCu_3Ti_4O_{12}$ BY AUTO-COMBUSTION TECHNIQUE"** submitted by **Mr. Sunil Patra**, to the National Institute of Technology, Rourkela in partial fulfillment of the requirements for the award of the degree of **Master of Technology in Ceramic Engineering** is a record of bonafide research work carried out by him under our supervision and guidance. His thesis, in our opinion, is worthy of consideration for the award of degree of Master of Technology in accordance with the regulations of the institute.

The results embodied in this thesis have not been submitted to any other university or institute for the award of a Degree.

Supervisor
Prof. R. Mazumder
Department of Ceramic Engineering
National Institute of Technology
Rourkela

Supervisor
Prof. S .K. Pratihar
Department of Ceramic Engineering
National Institute of Technology
Rourkela

Acknowledgement

It is with a feeling of great pleasure that I would like to express my most sincere heartfelt gratitude to **Prof. S. K. Pratihar** and **Prof. R. Mazumder,** Dept. of Ceramic Engineering, NIT, Rourkela for suggesting the topic for my thesis report and for their ready and able guidance throughout the course of my preparing the report. I thank you Sir for your help, inspiration and blessings. My very special thanks to P**rof. R. Mazumder** for his constant help throughout the project work.

I express my sincere thanks to **Prof. S. Bhattacharyya**, Head of the Department of Ceramic Engineering, NIT, Rourkela for providing me the necessary facilities in the department.

I would also take this opportunity to express my gratitude and sincere thanks to my honorable teachers **Prof. J. Bera, Dr. B. B. Nayak, Dr. S. K. Pal** and **Mr. A. Chowdhury** for their invaluable advice, constant help, encouragement, inspiration and blessings.

Submitting this thesis would have been a Herculean job, without the constant help, encouragement, support and suggestions from my friends, especially **Ganesh, Bhabani , Shyma, Rasmi, Sanjay, Ganga, Niroj, Smruti** for their time to help. Although it will be difficult to record my appreciation to each and every one of them in this small space; I will feel guilty if I miss the opportunity to thank, **R.P Rana, Y. Nayak, J.P.Nayak, S.K.Rout, S.Mohanty, H.Patra, A.Chakraborti** and others. I will relish your memories for years to come.

Last but not the least I would like to thank my parents and other family members for their support, blessing and affection. I would also express my sincere thanks to technical and non-technical staff members of Ceramic Engineering Department, N.I.T. Rourkela.

.

Date **SUNIL PATRA**

Abstract

$CaCu_3Ti_4O_{12}$ (CCTO) is a well known nonferroelectric material possessing high and nearly constant (room temperature to 300^oC) dielectric constant at 1 kHz. It is being widely used in the electronic industries to manufacture electronic components such as multilayer capacitor (MLCC), DRAMs, microwave devices, electronic devices in automobiles and aircrafts. The properties like high permittivity of $CaCu_3Ti_4O_{12}$ depend upon the particle size and powder morphology. The particle size and powder morphology of $CaCu_3Ti_4O_{12}$ depend on the different processing parameters that are temperature, heating rate, duration and atmosphere. Several powder synthesis processes have been tried for the synthesis of $CaCu_3Ti_4O_{12}$ among which solution combustion process have got enough emphasis now a days. $CaCu_3Ti_4O_{12}$ synthesized using combustion synthesis techniques possess high purity and close control of powder morphology, which will result in the desired microstructure and dielectric behavior. Under this context the present study was carried out to evaluate the effect of different processing parameters on the phase purity, particle size, and powder morphology of $CaCu_3Ti_4O_{12}$ and to study the effect of microstructure, sintering condition on the dielectric behavior of $CaCu_3Ti_4O_{12}$. The study includes the optimization of different process parameters (ammonium nitrate, citric acid, pH) for synthesis of phase pure CCTO powder following solution combustion route. The optimization of process parameters were based on the phase purity, crystallite size and density. The optimized ratio for synthesis of $CaCu_3Ti_4O_{12}$ was found to be 1:3:4:1.5:4 for $CaCO_3$,CuO, $TiO(NO_3)_2$, citric acid and ammonium nitrate respectively at pH 1.The powder morphology, particle size, densification behavior and dielectric behavior of the sintered samples has been studied. Increasing sintering time found to enhance the density. The dielectric study showed its dependence upon sintering time, grain size and density. Dielectric property increases with increase in sintering time and density. An attempt has also been made to study the effect of lanthanum substitution at A site on the properties of CCTO ceramics.

List of Figures

CONTENTS

Chapter1

INTRODUCTION

Introduction:

A great challenge in microelectronics is to decrease the size of passive components in general and capacitors in particular. For these reasons, there has been a considerable interest in the study of the giant dielectric permittivity of the cubic ABO_3 perovskite type $CaCu_3Ti_4O_{12}$ (CCTO) in the last decade. This material exhibits an extraordinarily high dielectric constant at room temperature of about 10^4 to 10^5 and good temperature stability in a wide temperature range from 100 to 600K [1,2]. Due to high dielectric constant, it is widely utilized to manufacture electronic components such as multilayer capacitor, electronic devices in automobiles and aircrafts [3]. They can also be applied to important devices such as DRAM (Dynamic Random Access Memory), microwave devices [4, 5, 6]. Many other materials also have a large dielectric constant, e.g., $Bi_{2/3}Cu_3Ti_4O_{12}$ (BCTO), $Y_{2/3}Cu_3Ti_4O_{12}$ (YCTO) and $La_{2/3}Cu_3Ti_4O_{12}$ (LCTO). All these large dielectric constant materials have similar dielectric behavior, i.e., they all exhibit a Debye-like relaxation and their dielectric constants are nearly independent of frequency and temperature well below the relaxation frequency. Among these, $CaCu_3Ti_4O_{12}$ has high dielectric constant due to internal barrier layer capacitance effect, which has been discussed below. Usually large dielectric constants are also found in ferroelectric materials e.g. $BaTiO_3$ and are related to atomic displacements within a noncentrosymmetrical structure. However, these perovskite materials exhibit high dependence on the temperature and the existence of the transition temperature is generally a problem for applications. The dielectric property of $CaCu_3Ti_4O_{12}$ can be tailored by modifying its structure using suitable dopants. Improved synthesis techniques have also enabled production of $CaCu_3Ti_4O_{12}$ powders with high purity and adjustable physical and chemical properties.

1.1. Structure of $CaCu_3Ti_4O_{12}$ (CCTO)

The structure of $CaCu_3Ti_4O_{12}$ is derived from the cubic perovskite (ABO_3) by an octahedral tilt distortion caused by size mismatch and the nature of the A cations. The TiO_6 octahedra tilt to produce a structure where three-quarters of the A sites have square–planar coordination and are occupied by Jahn–Teller Cu^{2+} ions [7]. The remaining quarters of the sites occupied by Ca and have 12 fold coordination.

CCTO is non-stoichiometric with respect to Cu content. The non-stoichiometry can be expressed as $CaCu_{3+y}Ti_4O_{12}$, where y is reported to vary from +0.1 [8] to - 0.15 [9].

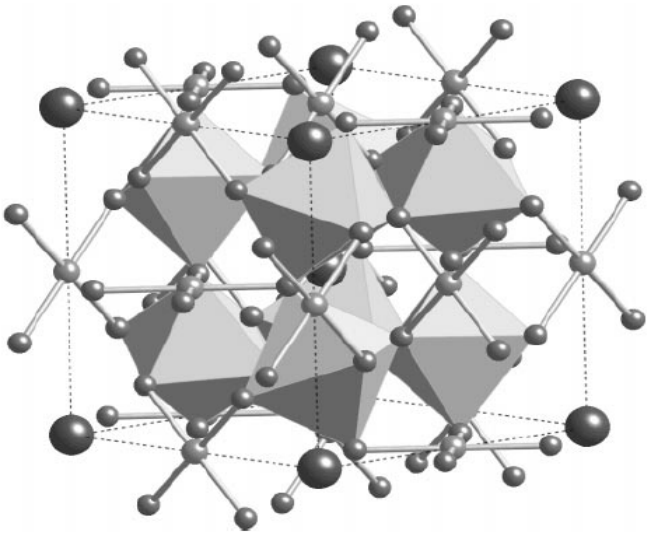

Fig.1.1. Structure of $CaCu_3Ti_4O_{12}$ shown as TiO_6 octahedra, Cu atoms bonded to four oxygen atoms, and large Ca atoms without bonds.

1.2. Origin of Dielectric behavior of CCTO

Recently, there has been considerable interest in $CaCu_3Ti_4O_{12}$ (CCTO), a material with a cubic perovskite related crystal structure, because of its unusual dielectric property. It exhibits an enormously large low-frequency dielectric permittivity (ε' is of the order of 10^4) in both forms of single crystals and ceramics at room temperature and keeps almost constant at low frequencies over the temperature range from 100 to 380 K. The dielectric constant (ε') drops rapidly to a value of about 100 with decreasing temperature or increasing frequency and shows the Debye-type relaxation behavior [10]. The characteristic relaxation frequency follows approximately the Arrhenius law [11, 2]. Nevertheless, neither a phase transition nor a detectable long-range crystal structure change has been observed in high-resolution x-ray and neutron powder diffractions and Raman-phonon measurement [11, 1]. Such behavior is scientifically interesting and technologically intriguing. So, the origin of large dielectric permittivity of $CaCu_3Ti_4O_{12}$ (CCTO) has attracted much attention. So far, several models have been proposed to explain the dielectric behavior and are quite controversial.

Subramanian *et al.* [1] had interpreted the high permittivity in terms of its intrinsic crystal structure, i.e., arising from the local dipole moments which are associated with off-center displacement of Ti ions, but the transition to a ferroelectric state is frustrated by the TiO_6 octahedral tilt being required to accommodate the Cu^{2+} square planar coordination. However, noticing the existence of high degree of twinning with small domains in the single crystal, they also suggested that these twin boundaries might act as the barrier layer

capacitance, thus offering a possible extrinsic explanation for the observed giant dielectric property. Ramirez *et al* [2] have proposed the collective ordering of local dipole moments as a cause of the unusually high dielectric response and explained the phenomenon by the highly polarizable relaxational excitations. Homes *et al.* [11] have suggested that the large change in dielectric constant at low temperature may be due to a relaxor like dynamical slowing down of dipolar fluctuations in nanosized domains, based on their optical measurement. Sinclair *et al.* [12,13] carried out an impedance spectroscopy measurement demonstrating that CCTO ceramics is electrically heterogeneous and consists of semiconducting grains with insulating grain boundaries and asserted that the giant dielectric phenomenon is attributed to a grain boundary (internal) barrier layer capacitance (IBLC) rather than an intrinsic property associated with the crystal structure. Cohen *et al.*[14] explained the giant dielectric permittivity of the single crystal arising from spatial inhomogeneity of local dielectric response. Lunkenheimer *et al* [15] pointed out that the apparently high values are due to contact-electrode depletion effect.

In summary, the giant dielectric constants have been variously attributed to: (i) the barrier layer capacitance arising at twin boundaries [1], (ii) disparity in electrical properties between grain interiors and grain boundaries [12], [16] and [17], (iii) space charge at the interfaces between the sample and the electrode contacts [18] and [15], (iv) polarizability contributions from lattice distortions [19], (v) differences in electrical properties due to internal domains [20], (vi) dipolar contributions from oxygen vacancies [21] and [22], (vii) the role of Cu off-stoichiometry in modifying the polarization mechanisms [8], (viii) cation disorder induced planar defects and associated inhomogeneity [23] or (ix) nanoscale disorder of Ca/Cu substitution giving rise to electronic contribution from the degenerate e_g states of Cu occupying the Ca site contributing to the high dielectric constant [24]. To date, the IBLC explanation of extrinsic mechanism is comparatively widely accepted.

1.2.1. Barrier-layer capacitors:

Barrier-layer capacitors are based on the limited reoxidation of a reduced composition. Although barrier layer capacitors are of little or no commercial significance, the principles upon which their manufacture and operation are based on are important. Most materials containing TiO_2, whether as a single phase or in combination with other oxides, become conductive on firing in reducing atmospheres. The ease of reduction is strongly affected by the other ions present: acceptor ions tend to inhibit reduction and donor ions tend to enhance

it [25]. In most cases a high resistivity can be restored by annealing in air or oxygen. Alternatively each conductive grain may be surrounded by an insulating barrier layer so that the dielectric property is dispersed throughout the ceramic.

1.2.2. Internal barrier layers:

The thinnest reoxidized layers, which result in very large effective permittivities, have properties similar in some respects to those of varistors. The thin layer behaves as Schottky barriers in the semiconducting surfaces of the grains which result in properties similar to those of two back-to-back diodes. Their working voltages are therefore limited to the range within which the current is low. In order to withstand higher voltages it is necessary to have a ceramic structure that comprises a number of such barrier layers in series between the electrodes. There must also be an intergranular component that allows the diffusion of oxygen and dopant ions to the crystallite surfaces during oxidation. The grain size in these units averages about 25 μm. Crystallites smaller than about 10 μm have a large fraction of their volume taken up by Schottky barriers and associated space charges that increase their resistivity, and if the crystals are larger than 50 μm there is the possibility that only a few crystals will separate the electrodes in some places, resulting in a greater likelihood of breakdown. Additions of small amounts (about 1%) of silica and alumina provide an intergranular layer that allows ionic movement and access to oxygen at high temperatures. Dysprosium or other donor ions are added to assist in the reduction process. Discs or other shapes are first fired in air to remove organic matter and then sintered in air to obtain the required level of crystal growth. A reducing atmosphere of carbon monoxide or hydrogen is then introduced. This is found to inhibit crystal growth and so cannot usually be combined with the sintering stage. After cooling, a boric oxide frit containing acceptor ions such as Cu, Mn, Bi or Tl is painted on the surfaces of the pieces which are then reheated in air to 1300–1400^{o}C. The acceptor ions diffuse along the grain boundaries and modify the surface properties of the crystallites in much the same way as the acceptors that protect dielectrics for base-metal-electroded multilayer capacitors. However, their precise behaviour has not been established since it is extremely difficult to determine the structure of the thin intergranular layers and their interfaces with the crystallites.

1.2.3. Requirement of getting Grain Boundary Capacitor:

1. Uniform grain size.
2. Continious grain boundary.
3. One species of grain.
4. Grain boundary thickness (t_{gb}) should be much less than the grain diameter (t_g).
5. Grain boundary permittivity should be equal to the grain permittivity.
6. Grain boundary resistance >> grain resistance.

The capacitance C_i of an individual element, assuming $t_g >> t_b$, is given by

$$C_i=\varepsilon_r\varepsilon_0 t^2_g/t_b$$

And that of a series connected column by

$$c_i=\frac{\varepsilon_r\varepsilon_0 t^2_g/t_b}{t/t_g}$$

The capacitance C per unit area is

$$C=\frac{\varepsilon_r\varepsilon_0 t_g}{t t_b}$$

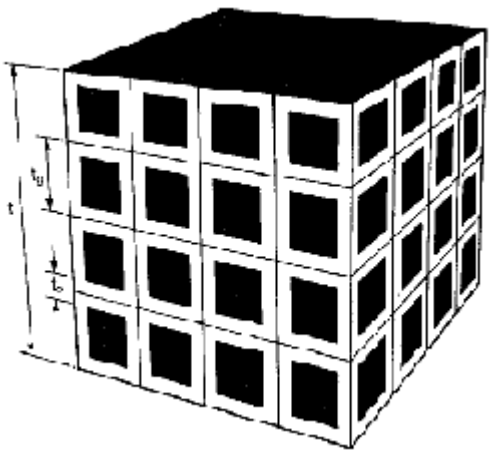

Fig.1.2.3.schematic diagram of a section through an internal – barrier layer capacitor.

since there are $1/t_g{}^2$ columns per unit area. It follows that the effective relative. Permittivity ε_{re} of the composite dielectric is

$$\varepsilon_{re} = \frac{\varepsilon_r t_g}{t_b}$$

Assuming t_g =50 μm, t_b =0.2 μm and ε_r =200, we obtain ε_r = 50 000. Values as high as this can be achieved in practice with tan d values of typically 0.03. Units based on $SrTiO_3$ are more stable with respect to field and temperature than those based on $BaTiO_3$. Their capacitance is only reduced by 5% under maximum d.c. field and their variation with temperature can be kept within +20% over a -20 to +85^{0}C range; their effective permittivity is 10 000–20 000. $BaTiO_3$ units have effective permittivities of up to 50 000.

1.3. Advantage of $CaCu_3Ti_4O_{12}$ over $BaTiO_3$

In the cubic perovskite structure encountered in $BaTiO_3$ above 120^{0}C, the Ti^{4+} cation is in a site of full cubic symmetry. With decreasing temperature, Ti^{4+} displaces toward one, then two and finally three oxygen anions, to produce, respectively, the tetragonal, orthorhombic and rhombohedral ferroelectric structures. The site symmetry for Ti^{4+} in $CaCu_3Ti_4O_{12}$ is much lower than that in cubic $BaTiO_3$; this greatly reduces the possibility of a ferroelectric phase transition based on the displacement of Ti^{4+} from the center of its octahedron. For example, the lack of a fourfold axis in the *Im3* space group for $CaCu_3Ti_4O_{12}$ eliminates the possibility of a transition to a tetragonal ferroelectric structure. The Ti^{4+} cations could displace off center, along their one threefold axis. However, this could not be a pure ferroelectric transition, because the displacements would actually occur along four different directions. Thus, we have in $CaCu_3Ti_4O_{12}$ a perovskite-type structure where polarizability and dielectric constant are enhanced by tension on the Ti-O bonds, but where a transition to a ferroelectric state is frustrated by the TiO_6 octahedra tilt structure that accommodates the square planar coordination of Cu^{2+}.

1.4. Synthesis of $CaCu_3Ti_4O_{12}$

The conventional solid state reaction method is widely used for synthesizing $CaCu_3Ti_4O_{12}$. The high impurity and poor powder characteristics, represented by a coarse particle size, wide particle size distribution, irregular particle morphology, and a high degree of inhomogeneity made this process unsuitable [26]. Other synthesis methods used to synthesize CCTO are wet-chemistry method [27], polymerized complex method [28], microwave heating [29], sol–gel method [30], pyrolysis [10], co-precipitation method [31].

. Sol-gel process use metal alkoxides as the starting materials, which are very expensive and extremely sensitive to the environmental conditions such as moisture, light and heat. Moisture sensitivity makes it necessary to conduct the experiment in dry boxes or clean rooms and also this method needs long heat-treatment times. Co-precipitation processes involve repeated washing in order to eliminate the anions coming from the precursor salts used, making the process complicated and very time consuming. Every synthesis route has advantages and disadvantages.

Researcher and scientists around the globe are working for the development of high purity phase pure $CaCu_3Ti_4O_{12}$ with improved powder morphology, which will provide enhanced dielectric constant with low loss. Several powder processing technique have been tried among them solution combustion seems to be promising one.

Solution combustion technique is a very useful technique widely used for the synthesis of phase pure single as well as complex oxide material. It is based on the redox reaction between the oxidant and fuel present in the precursor solution. The precursor solution consists of nitrates of the metal cation, a fuel and or a chelating agent in aqueous media, wherein the nitrates acts as the oxidant and provides and an environment for the combustion of the fuel. The precursor solution on dehydration formed a complex with the fuel and or the chelating agent leading to the formation of a viscous gel at the final stage of dehydration. This viscous gel on further heating swells with the decomposition of the nitrates present and finally burs out. The evolution of different fuels with or without the addition of chelating agent has been tried by different researches for synthesis of $CaCu_3Ti_4O_{12}$ powder through solution combustion technique.

Chapter2

LITERATURE

2.1 $CaCu_3Ti_4O_{12}$ Synthesis

Jianjun Liu et al. [27] had reported synthesis of fine crystalline $CaCu_3Ti_4O_{12}$ powder using wet-chemistry method at relatively low temperatures and a shorter reaction time. The pure-phase sample was obtained at 800 °C for 0.5 h and the grain size of a pellet sample sintered at 1030 °C for 4 hr has a homogeneous distribution in the range of 0.4–1.5 μm. This method start with a homogeneous liquid solution of cation ingredients mixed in stoichiometric ratio at the atomic scale. Therefore, pure samples at the nanometer scale could theoretically be obtained at lower temperature and a shorter reaction time than that afforded by solid-state reactions. In this method, the metal oxides are formed in the first heat-treatment step and CCTO is produced by a subsequent solid-state reaction.

Chivalrat Masingboon et al. [28] have synthesized nano-sized powders of $CaCu_3Ti_4O_{12}$ by a polymerized complex method followed by calcination in the temperature range 600-800^oC in air for 8 h. The diameter of the synthesized powders ranges from 30 to 100 nm. Sintering of the powders was conducted in air at 1100^oC for 16 h. The XRD study revealed that all sintered samples have a typical perovskite $CaCu_3Ti_4O_{12}$ structure with some amount of $CaTiO_3$ and CuO. SEM micrographs of the sintered $CaCu_3Ti_4O_{12}$ ceramics showed the average grain size of 10–15μm. The samples exhibit a giant dielectric constant of 10,000–20,000. This method was found useful due to its relative simplicity and usefulness for obtaining a homogeneous and fine powder precursor. But this method is still relatively complex, though, and need long heat-treatment times.

Jianjun Liu et al. [31] have synthesized the giant-dielectric-constant material CCTO by pyrolyzing an organic solution containing stoichiometric amounts of the metal cations, at a lower temperature and a shorter reaction time than that for conventional solid-state reaction. Synthesis from a solution affords intimate and homogeneous mixing of the metal ions at the atomic scale, thus reducing the diffusion path length required. A shorter diffusion length reduces reaction time and lower temperatures. The diameter of the powders ranges from 200 to 400 nm. The grain dimensions was increased to 2-3 μm after and sintered at 1050 °C for 4 h of the cold-pressed pellets. The samples exhibit a giant dielectric constant of 11500. However, this method still has the disadvantage that it involves handling chemicals in a glove box and refluxing of solutions.

Hongtao Yu et al. [29] have synthesized single-phase cubic perovskite $CaCu_3Ti_4O_{12}$ powders successfully by microwave heating with a relatively low energy consumption and short time, compared with conventional synthesis. This method is very clean and non-polluting and resulted in better reaction yields. XRD study suggests the formation of phase pure CCTO powder on calcinations at 800^oC for 2 hrs. The room temperature relative dielectric constant of 21400 at 1 KHz was reported at on sintering at 1100^oC for 3hrs.

Laijun Liu et al. [30,32] have synthesized the giant dielectric constant material $CaCu_3Ti_4O_{12}$ by sol–gel method using nitrate and alkoxide precursor. The phases, microstructures and impedance properties of final samples were characterized by X-ray diffraction, scanning electron microscopy and precision impedance analyzer. The dielectric permittivity of CCTO synthesized by sol–gel method was found three times larger than that synthesized by other low-temperature method as well as solid-state reaction method. The observed results were explained by internal barrier layer capacitor (IBLC) model of Schottky barriers at grain boundaries between semiconducting grains., A sol–gel process has shown considerable advantages, including excellent chemical stoichiometry, compositional homogeneity and lower crystallization temperature due to the mixing of liquid precursors on the molecular level [33,34] as compared with other techniques. Ion diffusing displacement is shortened in sol–gel process. The phase pure powders were obtained on calcinations at 900^oC for 1 hr. The dielectric constant of CCTO ceramics was found to be 35000 at 1 kHz in the sintered samples at 1060 C for 48 hrs.

S. F. Shao et al. [32] have prepared $CaCu_3Ti_4O_{12}$ ceramics by the conventional solid-state reaction method under various sintering temperatures from 1000 to 1120°C at an interval of 10 °C. Microstructures and crystalline structures were examined by scanning electronic microscopy and X-ray diffraction, respectively. It has been reported that the morphologies change significantly with the sintering temperature. Ceramic specimens prepared by this method have a good polycrystalline structure in spite of the different microstructures. The dielectric permittivity was found to increase with the sintering temperature and is closely related to the polycrystalline microstructure, particularly to the grain size. This suffers from the disadvantages of inhomogeneity and it also require repetitive grinding and firing at high temperatures and long reaction time.

P. Thomas et al. [35] have reported that the powders produced by the pyrolysis of the co-precipitated oxalates at 900^oC for 10 h yielded CCTO with $CaTiO_3$+CuO as the impurity phases. The phase-pure CCTO was obtained only after sintering the powders at 1050^0C. A

complex oxalate precursor was developed in order to avoid such difficulties in obtaining phase-pure CCTO powders at relatively lower temperatures. This method was found convenient for achieving chemical homogeneity, where the individual constituents intermix at the ionic level under controlled wet chemical conditions. The nanoparticles of CCTO with the crystallite size varying from 30 to 200 nm was reported to obtain at a temperature as low as 680^0C from the exothermic thermal decomposition of an oxalate precursor $CaCu_3(TiO)_4(C_2O_4)_8.9H_2O$. The powders derived from the oxalate precursor showed excellent sinterability, resulting in high-density ceramics which exhibited giant dielectric constants up to 40,000 (1 kHz) at 25^{o}C, accompanied by a low dielectric loss <0.07.

Julie J. Mohamed et al. [36] have synthesized $CaCu_3Ti_4O_{12}$ by the solid state technique. The sample was calcined at 900^{o}C/12 hrs and sintered at 1050°C/24 hrs. Increasing sintering temperature was found to enhance the density and secondary phase formation of Cu_2O. A clear grain boundary and dense microstructure were observed in the sintered samples. The results showed that the sample sintered at 1040°C/10 hrs yielded a uniform grain size with the highest ε_r (33,210).

B. Barbier et al. [31] have synthesized CCTO powders by a soft chemistry method (co-precipitation method). The sintered pellets showed a high room temperature dielectric permittivity (ε_r ~1.4×10^5) and relatively small dielectric losses (tan δ ~0.16) at 1 kHz. The study suggests that the high dielectric permittivity observed in this material are not related to an interface (electrode material) related mechanism but due to an internal barrier layer capacitor (IBLC) type. The samples prepared from the powder was found to exhibit a bimodal grain size distribution, with small grains of about 20 μm and large grains of size ranging 50 to 200 μm. It was also been investigated that nature of the electrode contact has no influence on the dielectric permittivity and the losses values of CCTO pellets. The dielectric permittivity strongly depends on the sample diameter while the dielectric losses remain constant whatever the diameter value.

Combustion synthesis using metal nitrates as oxidants and different organic compounds such as citric acid, α-alanine, glycine, urea and semioxamazide are used as fuel, is a useful technique for synthesis of high purity nano materials [37-42]. The solution combustion method is based on the advantage of the exothermic, fast and self-sustaining chemical reaction between the metal nitrates and a suitable organic fuel. Particle size and powder morphology of the product can be optimized by varying the different process parameters during the synthesis.

Jha et al.[43]. used, a polymeric precursor consisting of citric acid and ethylene glycol which on subsequent heat treatments led to pure $CaCu_3Ti_4O_{12}$ at 1000°C. On sintering further at 1000°C (20 h), the samples showed high density (98%) and the dielectric constant was found of the order of 3000 at 1 kHz. The dielectric loss was varied between 0.3 and 0.35 (till 100 kHz) beyond that it was found to increase sharply from 0.35 to 0.7 in the frequency range of 100-500 kHz. The dielectric constant was found to decrease with frequency. Microstructural study revealed that the grain size of the samples prepared from the polymeric citrate precursor route was much smaller (0.5-1.0 μm).

2.2. Factors affecting the properties of CCTO

Chih-Ming Wang et al. [26] had studied the dielectric properties of polycrystalline CCTO samples sintered at 1100°C in the dwell time range from 3 to 48 hrs prepared by conventional solid-state reaction technique. X-ray diffraction (XRD) patterns study showed no obvious change in crystal phase with various sintering times. The microstructural study indicated that the grain size was significantly increased with an increase of sintering time. The dielectric properties of CCTO ceramics are found very sensitive to processing.

Li et al. [44] studied the dielectric properties of polycrystalline $CaCu_3Ti_4O_{12}$ (CCTO) pellets sintered in the temperature range 1000-1200°C with impedance spectroscopy at frequency range of 10^2 to 10^7 Hz from 90 K to 294 K. A correlation has been suggested between the pair values of low frequency limit dielectric constant and the total resistivity and the sintering temperature. For example, the sample sintered at 1100°C demonstrates higher value of low frequency limit dielectric constant and lower value of total resistivity, while the sample sintered at 1000°C demonstrates lower values of low frequency limit dielectric constant and higher value of total resistivity. This correlation had been successfully explained by relating with the difference in grain size and grain volume resistivities of these two polycrystalline CCTO samples. Further, it has been suggested that donor doping of oxygen vacancies V_o' and V_o'' may be the reason to cause the difference in the grain volume resistivities of these two samples.

The effect of processing on the dielectric properties of $CaCu_3Ti_4O_{12}$ (CCTO) was studied by B.A. Bender et al. [45]. $CaCu_3Ti_4O_{12}$ has been prepared using conventional ceramic solid state reaction processing techniques. Powders mixed via mortar and pestle yielded CCTO with a room temperature permittivity of 11,700 and a loss of 0.047. However, attrition-milled powders led to CCTO with permittivities close to 100,000 which are in the

same range reported for single crystal CCTO. Increasing sintering temperature in the range from 990 to 1050°C led to an increase in both the dielectric constant (714 to 82,450) and loss (0.014 to 0.98). Increasing sintering times also led to substantial improvements in permittivity. Grain size and density differences were not large enough to account for the enhancement in dielectric constant. The colossal effective dielectric constant of close to one million at room temperature was measured after annealing in flowing argon at 1000°C. The study suggests that the primary factor affecting dielectric behavior is the development of internal defects. It suggested that higher defect concentration within the 'core' of a grain resulted in a higher conductivity of the core and therefore, higher effective dielectric constant but also higher loss. The giant permittivity of CCTO has been described by a model of conducting grains and insulating grains boundaries and the associated Maxwell–Wagner relaxation. However, this model requires that the insulating grain boundaries be thin, uniform, and robust to prevent percolation of the conducting grains [46-48].

Seunghwa Kwon et al. [49] had investigated the effects of cation stoichiometry on the dielectric properties of $CaCu_{3+x}Ti_{4+y}O_{12}$ (x = +0.06, 0, −0.06; y = +0.08, 0, −0.08) with varying cation stoichiometry prepared via the conventional solid state synthesis methods. X-ray diffraction study revealed that both Cu- and Ti-excessive CCTO compositions showed the evidence of a Cu_2O phase (with a low permittivity (ε ∼8)) in the interior regions of non-stoichiometric CCTO ceramics. In addition, a CuO phase was also observed on the outer surface layer on all compositions. It was proposed that these phases were formed through limited reoxidation of Cu_2O during cooling. Adams et al. [50] have also reported that a Cu_2O peak (∼36.5◦) was found on the surface of undoped CCTO sample after sintering at a slightly higher sintering temperature of 1115 ^{0}C. The study suggests that there might be a transition temperature where either CuO or Cu_2O secondary phase is favorable depending on sintering temperatures and times. In contrast, both Cu and Ti-deficient CCTO compositions showed

no secondary phases. Both Cu- and Ti-deficient CCTO showed higher dielectric constants than stoichiometric CCTO and larger dielectric losses than undoped CCTO. The lower dielectric constant is attributed due to the presence of the Cu_2O phase in both Cu- and Ti-excessive CCTO compositions.

Microstructure and dielectric properties of $CaCu_{3-x}Ti_4O_{12-x}$ (3 - x = 2.8–3.05) ceramics has been studied by Kang-Min Kim et al. [51]. The X-ray diffraction study showed that the powders (Cu/Ca = 2.8–3.05) heat-treated at 1140^0C for 12 h were indexed to the single CCTO phase. For simplicity, Cu/Ca (molar ratio) is denoted as C. The lattice parameters of CCTO powders with Cu/Ca ≥ 2.95 were slightly larger than the values for the CCTO powders with Cu/Ca ≤ 2.90. The microstructure of the CuO-deficient CCTO specimens (C2.80, C2.85, C2.90) sintered at 1140^0C for 12 h. showed uniform microstructures and no abnormally grown grains were found throughout the specimens and the average grain sizes were 4.7, 4.9, and 4.8 μm, respectively. However, CuO-enriched CCTO specimens sintered at 1140^oC for 12 h showed a coarse-grained microstructure. The microstructural evolution showed quite different behaviors according to the CuO content. Normal grain growth (NGG) behavior was observed at Cu/Ca ≤ 2.9, while abnormal grain growth (AGG) behavior was found at Cu/ Ca ≥ 2.95. AGG can be induced by two important parameters; interface structure [52,53,54] and the presence of an intergranular liquid phase [55-60]. TEM study in order to analyze the distribution and amount of the intergranular liquid showed that the location of the liquid phase always coincided with a grain boundary, and the liquid was identified as being a CuO rich phase by EDS analysis. It was reported that the amount of liquid increased with increasing CuO content in the specimen which indicates that the excess CuO added in the range of Cu/Ca ≥ 2.95 does not incorporate into CCTO lattice but increases the intergranular liquid phase. The ε'_{app} value was found to decrease in the liquid-abundant at a lower frequency (f = 10^1–10^4 Hz) while the samples with liquid-enriched specimen with little intergranular liquid shows a large ε'_{app} value even in the frequency range of 10^3–10^5 Hz. Moreover, the minimum loss tangent values increased significantly with increasing CuO content. This has been explained either by the compositional change in CCTO grains or by the variation in the intergranular phase. It has been suggested that the abnormal grain growth was advantageous to increasing apparent dielectric permittivity via a barrier layer mechanism. However, in order to achieve high apparent dielectric permittivity and low dielectric loss, the CuO-rich intergranular liquid phase should be minimized.

Jing Yang et al. [61] have studied the electrode/sample contact effects on the dielectric properties of the $CaCu_3Ti_4O_{12}$ ceramics. It was suggested that the colossal dielectric constant in CCTO is related partly originated from the electrode/sample contact effects which depends on the surface resistivity of the sample. When the surface resistivity of the ceramic is as high as 1.2×10^8 Ω cm, no obvious mobile space charges can be observed, and the dielectric properties of the sample are inert to the different metal electrodes and various sample thicknesses. However, after the surface resistivity is lowered to 3.1×10^7 Ω cm through post-annealing the sample in N_2 atmosphere at 750^0C, the dielectric properties of the sample become sensitive to the different types of contacts due to the mobile space charges. The dielectric constant of the sample with Pt electrode showed a significant enhancement (up to 5000 at 10 kHz) as compared to that of the sample with Ag electrode.

J. Lia, A.W. Sleight et al. [62] had suggested that the presence of internal resistive barriers in a crystal of the $CaCu_3Ti_4O_{12}$ material. The barrier was associated with the numerous twin boundaries. The presence of defects in the bulk phase was reported responsible for its conducting behavior. The presence of Ti on the Cu site was unexpected but very small amounts of Ti may be on the Cu site in CCTO. Depending on the synthesis temperatures the charge compensation took place by some reduction of Cu^{2+} to Cu^{1+}. On cooling, the Cu^{1+} would oxidize to Cu^{2+} giving up an electron to the Ti 3d band. So the bulk phase in CCTO becomes conducting.

S.F. Shao et al. [9] had investigated the effect of Cu-stoichiometry on the dielectric and electric properties of $CaCu_{3+y}Ti_4O_{12}$ (y = 0, ±0.025, ±0.05, ±0.1 and −0.15) ceramics prepared under various compositions by the conventional solid-state reaction method. X-ray diffraction study showed that all of the compositions had the good polycrystalline structures. Microstructural study suggests that Cu-deficiency samples exhibits the microstructures of uniform grain size distribution, whereas ceramics with Cu-stoichiometry and Cu-excess show microstructures of bimodal grain size distribution. Ceramics with Cu-stoichiometry shows the highest low-frequency dielectric permittivity and the lowest domain resistance. Any off-stoichiometry will result in the decrease of low-frequency dielectric permittivity and the increase of domain resistance. All the samples showed a very similar dielectric dispersion.

2.3. Role of doping

The dopant role on the electric and dielectric properties of the perovskite-type $CaCu_3Ti_4O_{12}$ (CCTO) compound is evidenced [63]. Impedance spectroscopy study showed

that the relevant permittivity value is attributed to sintered CCTO due to grain boundary (g.b.) effects. The g.b. permittivity value of the pure CCTO was found to be increased of 1-2 orders of magnitude by cation substitution on Ti site and/or segregation of CuO phase, while the bulk permittivity keeps values 90<r<180. Electrons were found responsible for the charge transport and a mean bulk activation energy of 0.07 eV was obtained at room temperature for all the samples studied. The g.b. activation energy ranges between 0.54 and 0.76 eV. A Defect models related to the transport properties has been proposed, supported by electron

paramagnetic resonance study. The grain boundary permittivity value $r_{,exp}$~3400 of pure

$CaCu_3Ti_4O_{12}$ found to be significantly increased up to ~150,000 by cation substitutions on Ti

site and/or segregation of CuO phase while the bulk permittivity keeps values 90<r<180, typical of many perovskitic compounds. It has been reported that a 2% substitution of Mn on Cu site results the decrease in permittivity value to about 100 in the temperature range 300–4.2K [64].

It has been observed that cationic substitutions and CuO presence weakly influence the bulk specific capacitance, but C_{gb} increases with increasing CuO. It is also evident that the highest C_{gb} value does not occur in the samples containing highest CuO wt %. The CuO residual phase increases the C_{gb} values possibly because of its segregation at the boundary, so contributing to an increase of disorder in that region. It has been suggested that only Cu deficiency causes a significant lowering of permittivity value with decreasing the Cu content in CCTO [8]. It has been observed that La 2%, V 2% and Cr 2% substitutions does not influence significantly C_{gb} with respect to the pure CCTO. Other substitutions show significant changes, in particular the greatest effect was obtained by substituting Fe, Co and Ni although CuO impurity phase was detected in the samples. Indeed, some kind of cationic substitution in CCTO can deeply modify the grain surface so creating high efficiency (capacitive) dielectric layers. It was observed that the lattice parameters depend both on

doping ion and its amount, while the bond length shows only minor variation. This study suggests that g.b. effects was responsible for the giant dielectric permittivity.

Nano-size $Ca_{1-\chi}La_{2\chi/3}Cu_3Ti_4O_{12}$ ($\chi = 0.00$, 0.05, 0.10, 0.15 and 0.20) precursor powders has been prepared via the sol–gel method and the citrate auto-ignition route and was then processed into micro-crystal $Ca_{1-\chi}La_{2\chi/3}Cu_3Ti_4O_{12}$ ceramics under heat treatment [65]. Characterization of the as-obtained ceramics with XRD and SEM showed average grain sizes of ~1–2 μm, indicating La^{3+} amount to have little impact on grain size. The room-temperature dielectric constant of the $Ca_{1-\chi}La_{2\chi/3}Cu_3Ti_4O_{12}$ ceramics sintered at 1000°C was of the order of 10^3–10^4 despite the variation of χ values. Compared with $CaCu_3Ti_4O_{12}$, La^{3+}-doped $CaCu_3Ti_4O_{12}$ showed a flatter dielectric constant curve related to frequency. It was found that the loss tangent of the $Ca_{1-\chi}La_{2\chi/3}Cu_3Ti_4O_{12}$ ceramics was less than 0.20 in ~600–10^5 Hz region, which rapidly decreased to a minimum value of 0.03 by La^{3+}doping with $\chi = 0.05$.

Shuhua Jin et al [65] investigated the effect of La-doping on the properties of $CaCu_3Ti_4O_{12}$ dielectric ceramics. Nano-size $Ca_{1-x}La_{2x/3}Cu_3Ti_4O_{12}$ (x = 0.00, 0.05, 0.10, 0.15 and 0.20) precursor powders were prepared via the sol–gel method and the citrate auto-ignition route. From DTA curve they found that the main endothermic peaks appeared at 120 ^{0}C and exothermic peaks at 380^{0}C due to evaporation of the absorbed water and the combustion of some organic contents respectively , are shifted towards the lower temperature as x values were increased (that is with the doping of La^{3+}.). From XRD they found that no independence of $La(NO_3)_3$ phases has been observed for samples with x = 0.05– 0.20, which indicated that La^{3+} did almost not influence the crystalline structure. And also found that increasing the x value, the lattice peaks of the $Ca_{1-x}La_{2x/3}Cu_3Ti_4O_{12}$ system linearly decreased. The XRD patterns also presented that the average grain size of samples at x = 0.00–0.20 was 1–2 μm estimated by Scherrer's equation [66]. From SEM images of the $Ca_{1-x}La_{2x/3}Cu_3Ti_4O_{12}$ ceramics with different x values sintered at 1000^{0}C for 2 h, it can be seen that the specimens displayed a homogeneous microstructure with an average grain size of about 1–2 μm. The ϵ_{max} values became gradually smaller as the x value increased from 0.05 to 0.15. However, as x increased up to 0.20, the ϵ_{max} value became considerably high, which was almost higher than that of sample with x = 0.00. Cation distortions may exist and be attributed to this phenomenon [13]. In addition, the curves about ϵ values of samples with

x = 0.05–0.15 were fairly flat while the curves of x = 0.20 and x = 0.00 were much steeper. Over the frequency range from 10^2 to 10^5 Hz, tan α values at x = 0.05–0.20 were small and almost not varied with frequency and the tan α values were less than 0.20 in 600–10^5 Hz region. However, the tan α value at x = 0.00 varied strongly with the increase of frequency. For samples with x = 0.05–0.15, the tan α values became higher as the concentration of La^{3+} grew up. They got that the conductivity σ values of $Ca_{1-x}La_{2x/3}Cu_3Ti_4O_{12}$ ceramics did not show any regulation with x values. There was a tendency of σ to increase with the increase of frequency when it was higher than 100 kHz.

Alok Kumar Rai et al [67] had examined the dielectric properties of lanthanum-doped $Ca_{(1-3x/2)}La_xCu_3Ti_4O_{12}$ (x = 0.10, 0.20 and 0.30) synthesized by semi-wet route. XRD study confirmed the formation of monophasic compounds when calcined at 900^0C for 6 hr. The lattice parameter as determined from least square refinement method was found to increase with increase in lanthanum concentration. The increase in lattice parameter is attributed to the higher ionic radius of La^{3+} as compared to Ca^{2+}. The average grain size was found to be in the range 2-4 μm. The average grain size was found to decrease with increase in lanthanum doping as compared to undoped CCTO which is also supported by Kobayashi and Terasaki [68]. The dielectric constant as well as the dielectric loss of the samples was found to decrease with increasing lanthanum concentration.

. S. F. Shao, et al [69] had reported high permittivity and low dielectric loss in ceramics with the nominal compositions of $CaCu_{3-x}La_{2x/3}Ti_4O_{12.}$ $CaCu_{3-x}La_{2x/3}Ti_4O_{12}$ samples were prepared by the conventional solid-state reaction technique. $CaCu_{2.9}La_{0.2/3}Ti_4O_{12}$ ceramics sintered at 1050°C for 20 h showed the high dielectric permittivity of 7500 with weak frequency dependence below 1 MHz, the low dielectric loss less than 0.05 in the wide frequency range of 120 Hz–200 kHz. It has been suggested that $CaTiO_3$ secondary phase due to Cu deficiency and La doping plays the important roles in the observed excellent dielectric properties in $CaCu_{3-x}La_{2x/3}Ti_4O_{12}$ ceramics. Cu deficiency in CCTO ceramics was confirmed to result in microstructures of small and uniform grain sizes and resistivity increases [9]. It has also been reported that the partial La substitution at the Ca site in CCTO ceramics lead to changes of grain resistivity and/or grain boundary resistivity [70,71,72].. CCLTO ceramics showed much regular and dense polycrystalline microstructures, the average grain size decreases and the porosity increases with the La concentration. The microstructures of small

and uniform grain sizes observed in CCLTO ceramics were considered to be closely associate with the Cu deficiency [9]. The dielectric properties and the complex impedance of CCTO ceramics have been well investigated and explained by the internal barrier layer capacitance effect. Since R_{gb} is usually significantly larger than R_b. It has been suggested that the $CaTiO_3$ secondary phase acts as the barrier layers at the grain boundaries, which contribute largely to the excellent dielectric properties observed in the CCLTO ceramics. La^{3+} ions have nearly the same radius as Ca^{2+} ions and are much larger than Cu^{2+} ions, hence it prefers to enter into Ca sites rather than into Cu sites to form either $La_{2/3}CaCu_3Ti_4O_{12}$ [73,74,1] or $(Ca_{1-y}La_{2y/3})Cu_3Ti_4O_{12}$ [75]. As a result, the compositions are apparently Cu deficiency from the stoichiometric formula of $CaCu_3Ti_4O_{12}$, which then easily causes the occurrence of $CaTiO_3$ segregation.

Chapter3

Objective

Objective

Miniaturization requires high permittivity materials which is stable over a wide range of temperature, with adequate control over physical and chemical properties. $CaCu_3Ti_4O_{12}$ with a high permittivity is essential to enhance the volumetric efficiency of multi-layer ceramic capacitors (MLCCs), especially for the high volumetric efficiency of electronic components which depends on particle size. The increasing in size of particles leads to the enhancement of their permittivity because larger grains formation leads to a higher value of the dielectric constant, supported by internal boundary layer capacitor model. This enhancement results from off-center displacement of Ti ions, from the centrosymmetric position within the TiO_6 octahedron. Increase in dielectric permittivity is also due to by internal barrier layer capacitor effect between semi-conducting grain and insulating grain boundary. This effect can be enhanced by the La substitution on A site due to formation of $CaTiO_3$ as a secondary phase at the grain boundary.

Several synthesis routs namely solid state synthesis, wet-chemical method, polymerized complex method, microwave heating, sol–gel method, pyrolysis, co-precipitation has been tried to synthesize the material. Solid state synthesis route is widely used to prepare the powder, however it requires long heat-treatment times. Pyrolysis has the disadvantage that it involves handling chemicals in a glove box and refluxing solutions. In sol-gel process use metal alkoxides as the starting materials, which are very expensive and extremely sensitive to the environmental conditions such as moisture, light and heat. Co-precipitation processes involve repeated washing in order to eliminate the anions coming from the precursor salts used, making the process complicated and very time consuming.

Among the several alternative, combustion synthesis is a useful technique for synthesis of high purity nano materials. Because the advantages of auto-combustion route over other mentioned synthesis routes are low processing cost, energy efficiency and high production rate. This method is a simple method for oxides synthesis and has been used to produce homogeneous, crystalline nanopowders but its success depends on the correct understanding of the influence of the synthesis process parameters. Research revealed that particle size and

powder morphology of the product can be tailored by varying the different process parameters during the synthesis.

The objective of the present work is to synthesis of phase pure $CaCu_3Ti_4O_{12}$ and lanthanum doped $CaCu_3Ti_4O_{12}$ and to study the dielectric behavior of the samples prepared from this powder. The specific objectives of the present study are as follows:

1. Optimization of different process parameters that are ammonium nitrate, citric acid and pH for synthesis of phase pure $CaCu_3Ti_4O_{12}$ and lanthanum doped $CaCu_3Ti_4O_{12.}$
2. To study the dielectric behavior of pure $CaCu_3Ti_4O_{12}$ as a function of microstructure.
3. To study the dielectric property of $CaCu_3Ti_4O_{12}$ as a function of lanthanum doping.

Chapter4

EXPERIMENTAL PROCEDURE

4.1. Powder Synthesis

$CaCu_3Ti_4O_{12}$ powder has been synthesized following combustion synthesis technique. Combustion synthesis is generally used to synthesis phase pure multicomponent single phase material. The combustion technique is based on redox reaction between a fuel and oxidant present in the precursor solution. Generally citric acid, urea, ethyl glycol etc. are used as the fuel and nitrates of different metals are used as the oxidant. The fuel used or some other chelating agents like EDTA, acetic acid etc. used along with the fuel makes complexes with the metal ions present in the precursor solution. This complex on dehydration produces a viscous gel which on further heating self ignites with the evolution of huge amount of gases. This leads to the development of porous floppy ash. Fine phase pure powder can be obtained on further calcination of the ash at high temperature. Several process parameters have been reported to control the complex formation and decomposition / self ignition of the gel. In the present study $CaCu_3Ti_4O_{12}$ powder has been prepared using combustion synthesis technique. Citric acid was used as the fuel. The other precursors for the metal cation were $TiO(NO_3)_2$, $CaCO_3$, CuO , wherein the $TiO(NO_3)_2$ had been prepared in house. The other constituent of the precursor solution was ammonium nitrate. The different experimental techniques used during the present study have been discussed below:

4.1.1 Preparation of $TiO(NO_3)_2$ solution and its estimation

Titanium dioxide (TiO_2) is generally insoluble in mineral acid, however TiO_2 reacts with the sulphuric acid (H_2SO_4) and formed titanium oxysulphate ($TiO(SO_4)$). The formation of $TiO(SO_4)$ can be enhanced with the addition of ammonium sulphate $(NH_4)_2SO_4$ addition. The reaction can proceeds in the forward direction in hot condition. The preferred temperature was reported to be 80-90^oC. The preparation of $TiO(NO_3)_2$ solution has been discussed as follows. Weighted amount of TiO_2 [Merck], and $(NH_4)_2SO_4$ [Merck], were added to concentrate H_2SO_4 [Merck], in the ratio 1:6:12ml. The mixed suspension was heated on hot plate with constant and vigorous stirring until a solution was obtained. The dissolution reaction may be written as follows:

$$TiO_2 + H_2SO_4 = TiO(SO_4) + H_2O \quad \text{.....(4.1)}$$

The solution was then diluted with addition of distilled water in an ice bath. Ammonium hydroxide (NH_4OH) [Oster] was added to chilled solution, wherein a white precipitate was formed. The possible reaction for the formation of precipitate may be written as

$$TiO(SO_4) + 2NH_4OH = TiO(OH)_2 \downarrow + ((NH_4)_2SO_4 \quad \text{.....(4.2)}$$

The precipitate was washed repeatedly to make sulphate free. Then, the washed white precipitate was dissolved in dilute nitric acid (HNO_3) [Merck], (HNO_3: H_2O = 1:1). The possible reaction may be written as

$$TiO(OH)_2 + 2HNO_3 = TiO(NO_3)_2 + 2H_2O \quad \text{..... (4.3)}$$

Thus the $TiO(NO_3)_2$ had been prepared for the present study. TiO_2 content of the $TiO(NO_3)_2$ solution thus prepared has been estimated using gravimetric technique.

4.1.2. Combustion Synthesis of $CaCu_3Ti_4O_{12}$ Powder

$CaCu_3Ti_4O_{12}$ powder was prepared using citrate-nitrate gel combustion technique. Precursors used for synthesis were as prepared $TiO(NO_3)_2$, $CaCO_3$, Citric acid monohydrate $C_6H_8O_7$ [Merck] and Ammonium nitrate NH_4NO_3 [Merck] . Proportionate amount of above precursors were taken together. pH of the solution was adjusted using NH_4OH.The solution was placed on the hot plate. The temperature of the hot plate was then kept in the range of 80–90^{0}C. Dehydration of the homogeneously mixed solution during heating caused the development of a viscous gel. This gel on further heating self ignites followed by swelling of the gel. This ignition product ash was voluminous and floppy in nature. This ash on calcination yield phase pure $CaCu_3Ti_4O_{12}$ powder. The flow chart for the powder synthesis is given in Fig. 4.1

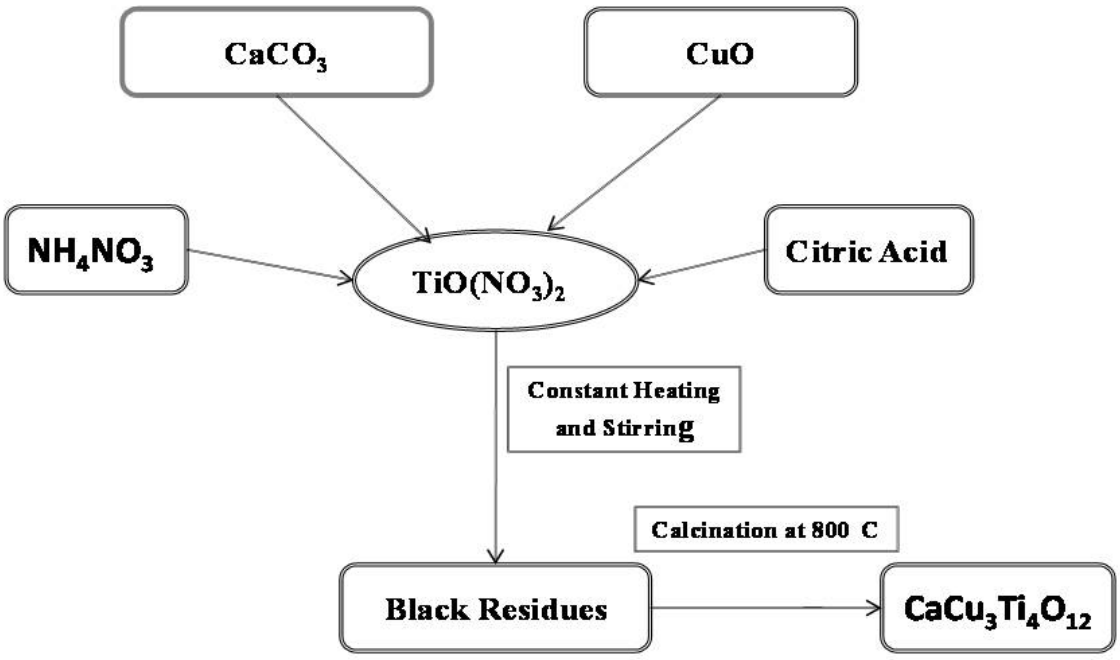

Fig. 4.1 Flow chart for the powder synthesis

4.2. Powder Characterization

4.2.1 Thermal decomposition behavior of the gel

Thermal decomposition behavior of the gel has been studied using Netzsch (STA 449C) DSC/TG. The DSC/TG patterns were collected as a function of temperature up to 900^{o}C under N_2 atmosphere. The heating rate was 10^{o}C/min. in N_2. Alpha alumina was used as reference material.

4.2.2 Phase analysis of calcined powder

The phase evolution of calcined powder as well as that of sintered samples was studied by X-ray diffraction technique (Philips PAN analytical, The Netherland) using CuKα radiation. The generator voltage and current was set at 35 KV and 25 mA respectively. The samples were scanned in the 2θ ranges 15 to 70^{o}C range in continuous scan mode. The scan rate was 0.02^{o}/sec.

Phases present in the sample has been identified with the search match facility available with Philips X'pert high score software. The crystallite size of the calcined powders was determined from X-ray line broadening using the Scherrer's equation [17] as follows:

$$t = 0.9\lambda/B\cos\theta \quad \ldots\ldots\ldots\ldots \quad (4.4)$$

Where, t = crystallite size,

λ = wavelength of the radiation,

θ = Bragg's angle and

B = full width at half maximum

4.2.3. Particle Size Analysis

A laser diffraction method with a multiple scattering technique has been used to determine the particle size distribution of the powder. It was based on Mie-scattering theory. In order to find out the particles size distribution the $CaCu_3Ti_4O_{12}$ powder was dispersed in water by horn type ultrasonic processor [Vibronics, model:VPLP1].Then experiment was carried out in computer controlled particle size analyzer [ZETA Sizers Nanoseries (Malvern Instruments Nano ZS)] to find out the particles size distribution.

4.2.4. Preparation of Bulk Sample

Calcined powder was mixed with 3 wt. % PVA (Poly Vinyl Alcohol) binder with the help of mortar and pestle. The binder mixed powder was compacted to give a desired shape for further characterization. The binder mixed powders were pressed uniaxially in a HC-HCr die into cylindrical pellets (12 mmΦ, 3mm high). The uniaxial pressing was done at 270MPa in a hydraulic press (10 T, Soillab testing instruments, India). A holding time of 90seconds was given for pressing of each sample. The pressed green compacts were sintered in air with a heating rate

of 3°C/min at the temperature ranges 950-110^{o}C with a holding time of 4 hours in electrical furnace. The bulk density and apparent porosity of the sintered specimen were measured by Archimedes Principle.

4.3. Densification study

The densification behavior and sintering kinetics have been studied using NETZSCH (DL 402C) Dilatometer in the temperature ranges 30 to 1000^{o}C under constant rate heating (CRH technique). The heating rates were 3^{o}C, 10^{o}C and 15^{o}C per minute.

4.4. Microstructure Analysis

Microstructure of sintered pellets has been studied using Scanning Electron Microscope (JEOL - JSM 6480LV). The generator voltage was 15 kV. Polished samples were prepared with Buehler, Ecomet 3; Automet 3 untill mirror finished is attained. The polished surface of the sample was then thermal etched at a temperature 50^{o}C below the sintering temperature for half an hour.

4.5 Dielectric measurement

Dielectric measurement sample have been prepared by electroding with silver paste. The silver paste coated samples were cured at 550^{o}C for half an hour. Dielectric measurement has been carried out using Solatron S1 1260 Impedance /Gain-phase analyzer with Solatron 1296 dielectric interface. The frequency range for the dielectric measurement was varied in the range of 10Hz to 1MHz. Dielectric behavior has also been studied as a function of temperature.

Chapter5

RESULTS AND DISCUSSION

5.1. Optimization Process Parameters for Synthesis of Phase pure Calcium Copper Titanate

Combustion synthesis is an easy and convenient method for the preparation of a variety of advanced ceramics and nanomaterials. This technique based on the principles of the propellant chemistry in which a thermally induced redox reaction takes place between an oxidant and a fuel. By this method it is possible to produce monophasic nanopowders with homogeneous microstructure, at lower temperatures or shorter reaction times, if compared with other conventional methods like solid-state synthesis. In this method, citric acid used as a fuel and metal nitrates are used as metal and oxidant source. Citric acid acts as a chelating agent as well as the fuel. Citric acid/metal nitrates ratio (C/M) was varied between 1 and 4. Ammonium nitrate was added to regulate the fuel/oxidant ratio (F/O), represented by the citric acid/total nitrate ions ratio, which was varied between 0.4 and 1.6. Finally ammonia solution (30 wt.%) was slowly added to adjust the pH at the desired value.

Optimization of different process parameters namely ammonium nitrate, citric acid, and pH on the phase formation of pure $CaCu_3Ti_4O_{12}$ powder have been discussed below.

5.1.1. Optimization of NH_4NO_3

Citrate ion acts as reductant and nitates ion act as oxidant in citrate-nitrate combustion process. Nitrates provide an in-situ environment for decomposition of organic components through the enhancement of oxidation rate. NH_4NO_3 is a strong oxidizing agent and added in the citrate nitrate combustion technique to increase the intensity of the oxidation-reduction reaction. A complete reaction between the mixture compounds was reached when there exists an optimum oxidizer/reducer ratio of nitrates to citrates. Molar ratio of NO^- : CA had influenced the appearance and purity of the final product [76]. Thus the optimization of NH_4NO_3 has a great importance for the process. The possible equation for combustion reaction may be written as follows:

$$CaCO_3+CuO+TiO(NO_3)_2+C_6H_8O_7+NH_4NO_3 \longrightarrow CaCu_3Ti_4O_{12}+CO_2+N_2+H_2O$$

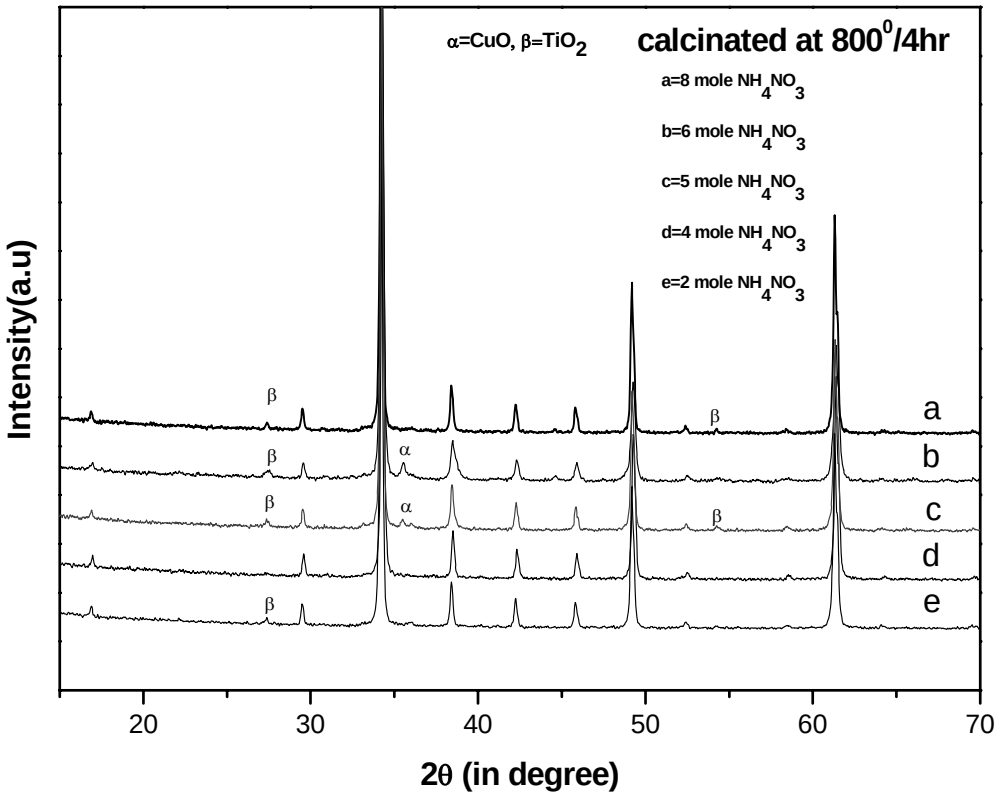

Fig 5.1.1 XRD pattern of $CaCu_3Ti_4O_{12}$ powder prepared with $CaCO_3$: CuO: $TiO(NO_3)_2$: $C_6H_8O_7$ = 1:3:4:1.5 calcined at 800°C as a function of NH_4NO_3 content.

The effect of NH_4NO_3 on the combustion has been studied from the phase formation and densification behavior of the powder (calcined at 800°C) prepared with the optimized batch $CaCO_3$: CuO: $TiO(NO_3)_2$: $C_6H_8O_7$ = 1:3:4:1.5, wherein the NH_4NO_3 has been varied from 2 to 8 mole. It has been observed that the intensity of the oxidation/reduction reaction decreases with increase in NH_4NO_3 content in the combustion solution. XRD patterns of the powder calcined at 800°C thus produced have been presented in Fig.5.1.1 as a function of NH_4NO_3 contain. It could be seen from the X-ray diffractogram that the powder prepared with 4 mole NH_4NO_3 crystallizes only pure $CaCu_3Ti_4O_{12}$ at 800°C for 4hr, whereas that prepared with 2, 5, 6, and 8 mole NH_4NO_3 contains some extra peaks of CuO, TiO_2 and $CaTiO_3$. The presence of impure phases in 2, 5, 6,

and 8 mole NH_4NO_3 containing batch composition is due to deviation of stoichiometric fuel/oxidant ratio as a result the stability of metal-citrate complex decreases and so the intensity of combustion was found to decrease.

5.1.2 Optimization of citric acid

Citric acid used in the batch formulation acts as the fuel as well as the chelating agent. An attempt has been made to optimize the amount of citric acid required for the formation of phase pure $CaCu_3Ti_4O_{12}$ (CCTO) at lower temperature. The different constituents of the batch were $CaCO_3$: CuO: $TiO(NO_3)_2$: $C_6H_8O_7$: NH_4NO_3 = 1:3:4:x:2, wherein the x has been varied from 1-2.5. It has been observed that the stable gel was formed only with 1.5 mole of citric acid. In all the batches prepared other amount of citric resulted precipitation before combustion of the gel. Thus the optimum amount of citric acid was found to be 1.5 mole.

5.1.3 Optimization of pH

pH of the precursor solution has a significant influence on the decomposition and combustion behavior of gel precursors which determine the properties of final product. It is known that citrate–nitrate stoichiometry in the precursor solution is the primary factor in controlling the reaction enthalpy in such a redox reaction. The increase in pH would lead to an increase in NO_3^- ion content and increases the decomposition rate because the nitrate ions provide an in situ oxidizing environment for the decomposition of organic components [77].

Effect of pH has been studied from the phase formation behavior of the $CaCu_3Ti_4O_{12}$ powder prepared from the batch $CaCO_3$: CuO : $TiO(NO_3)_2$: $C_6H_8O_7$: NH_4NO_3 = 1:3:4:1.5:4, wherein the pH was varied from 1 to 5. Phase formed and purity of the phase was examined from the analysis of the X-ray diffraction patterns of such powders calcined at 800^oC for 4 hr. It was observed that the gel formation prior to combustion occurs in the batches prepared with pH 1 and 3 whereas it causes precipitation when the batch was prepared at pH 5.

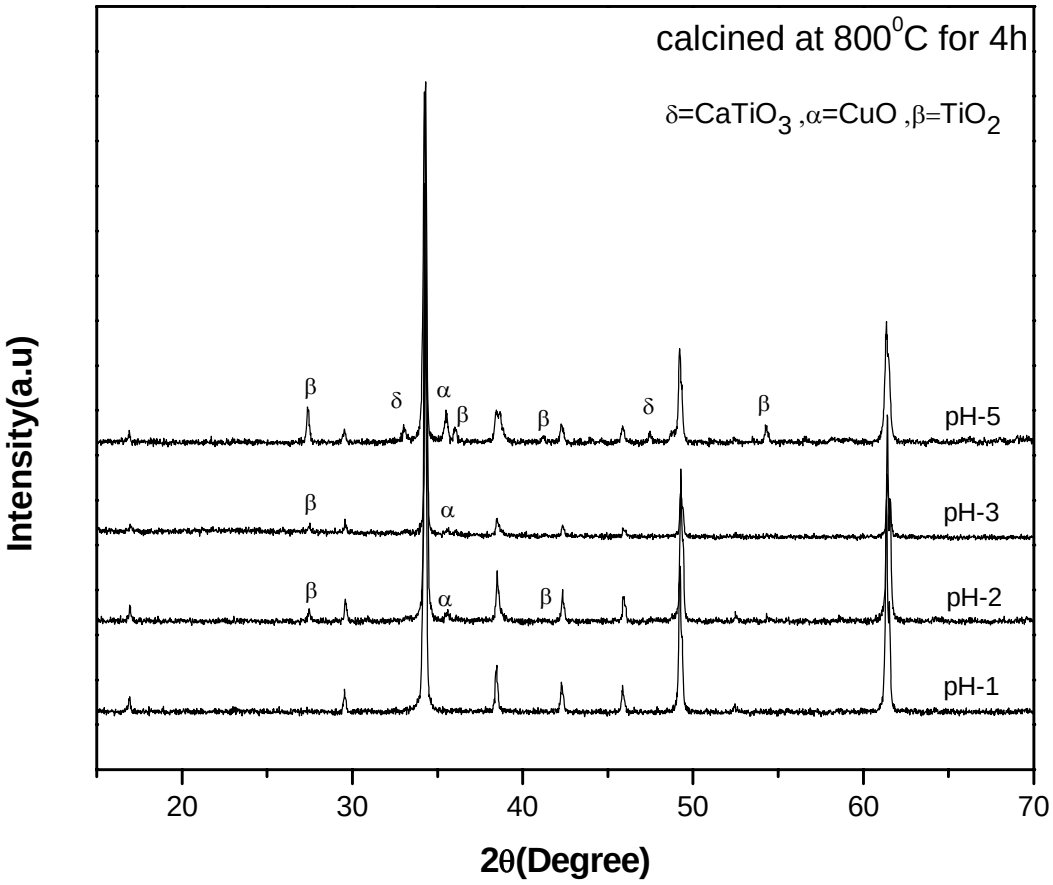

Fig 5.1.3 XRD pattern of $CaCu_3Ti_4O_{12}$ powder prepared with CaCO3 :CuO: $TiO(NO_3)_2$:NH_4NO_3: C_6H_8O7 = 1:3:4:4:1.5 calcined at 800^{o}C as a function of pH of the precursor solution.

Figure 5.1.3 shows the XRD pattern of the 800^{o}C calcined powder as a function of pH. It could be observed that the powder prepared at low pH (pH 1 -3) have pure $CaCu_3Ti_4O_{12}$ phase at 800^{0}C. On the other hand pure $CaCu_3Ti_4O_{12}$ phase could not formed at high pH (pH>2) at 800^{o}C because of precipitation during dehydration process prior to combustion. The low pH reduces the esterification of mixed-metal CA complex and enhances the bonding between Ca ions and Ti–CA complex, leads to the formation of more stable complex [78]. This stable complex formation in turn resulted the formation of phase pure $CaCu_3Ti_4O_{12}$ when synthesized at low pH. On the other hand the solution with low pH, the Ti–CA complex might retard the bonding of Ca ions to Ti–CA complex resulted the possibility free Ca ions in the dehydrated solution. This causes the precipitation at the final stage of dehydration when the powder was prepared at high pH. The crystallite size calculated for pure $CaCu_3Ti_4O_{12}$ phase prepared at pH 1 was 66 nm when

calcined at 800^0C. Thus it was suggested that the optimized batch for synthesis of pure highly sinterable $CaCu_3Ti_4O_{12}$ should be CaCO3 : CuO : $TiO(NO_3)_2$: $C_6H_8O_7$: NH_4NO_3 = 1:3:4:1.5:4, wherein the pH of the precursor solution should be maintained at pH 1.

5.2 Synthesis of $CaCu_3Ti_4O_{12}$

$CaCu_3Ti_4O_{12}$ powder have been synthesized from previously optimized batch $CaCO_3$: CuO : $TiO(NO_3)_2$: $C_6H_8O_7$: NH_4NO_3 = 1:3:4:1.5:4, at pH 1. The decomposition behavior of the gel, phase evolution of the powder, sintering behavior, microstructure development and dielectric properties etc. have been discussed as follows.

5.2.1 Thermal decomposition behaviour of the gel

The DSC/TG curve of the as prepared gel is given in Fig. 5.2.1. The DSC curve shows five exothermic peaks at 184^0C, 188.5^{o}C, 236^{o}C and 389.5^{o}C, 422^0C respectively. The TG trace indicates there were three major different distinct stages of weight losses over the temperature range 37-188^{o}C, 208–254^{o}C and 362-453^{o}C respectively. The weight loss in the low temperature region (37-188^{o}C) is 67.45%, where as that in the intermediate temperature (208–254^{o}C) region it is only 12.6% and 9.23% in the high temperature (362-453^{o}C) region. Decomposition of citric acid and partial decomposition of precursor in the present material will lead to combustion. There is a very sharp weight loss in the TGA curve in the temperature range from 37 to 188^0C , which may correspond to the decomposition of gel. A small weight loss in the temperature range 208–254^{o}C may be due to elimination of decomposition of excess citric acid [67]. And the weight loss in the temperature range 362-453^{o}C may be due to the loss of the carbonaceous materials formed after decomposition of the citrate nitrate gel. This major weight loss in TGA is also supported by an intense exothermic peak in the DSC curve.

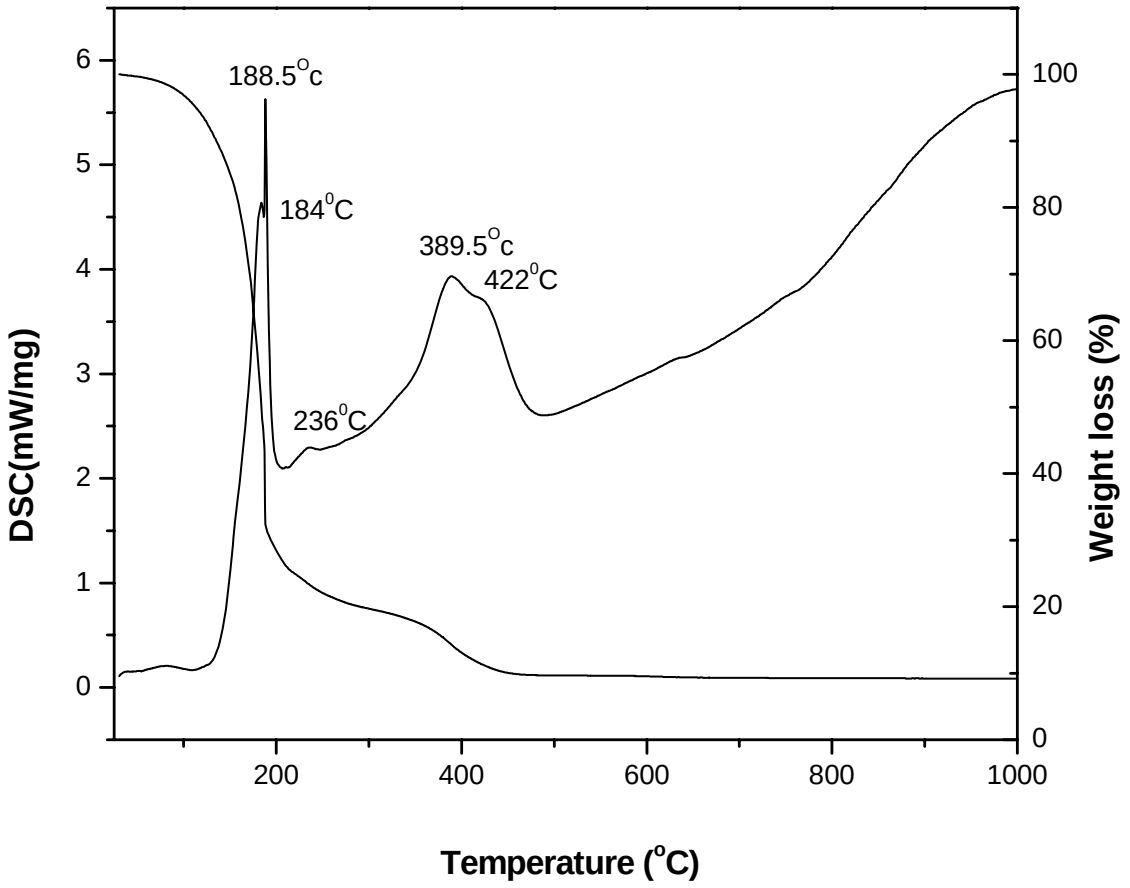

Fig 5.2.1 DSC/TG plot of the gel prepared from CaCO3 : CuO : $TiO(NO_3)_2$:$C_6H_8O_7$: NH_4NO_3 = 1:3:4:1.5:4, at pH 1.

5.2.2 Phase evolution of calcined CCTO powder

Figure 5.2.2 shows the XRD patterns of CCTO powder as a function of calcination temperature in the temperature ranging 700 – 800°C. Powder calcined at 700 and 750°C shows formation of $CaCu_3Ti_4O_{12}$ with a extra peak which we could not able to identify may be some intermediate compound fromed from the decomposition of the polymeric gel. Powder calcined at 800°C shows phase pure $CaCu_3Ti_4O_{12}$ without any impurity phases. $CaCu_3Ti_4O_{12}$ formation at a low temperature may be the direct result of combustion processes in which the formation of thermodynamically non-equilibrium products occurs or may be due to the smaller crystallite size of the powder. Average crystallite size calculated using Scherer's formula was found to be 66 nm when the powder calcined at 800°C.

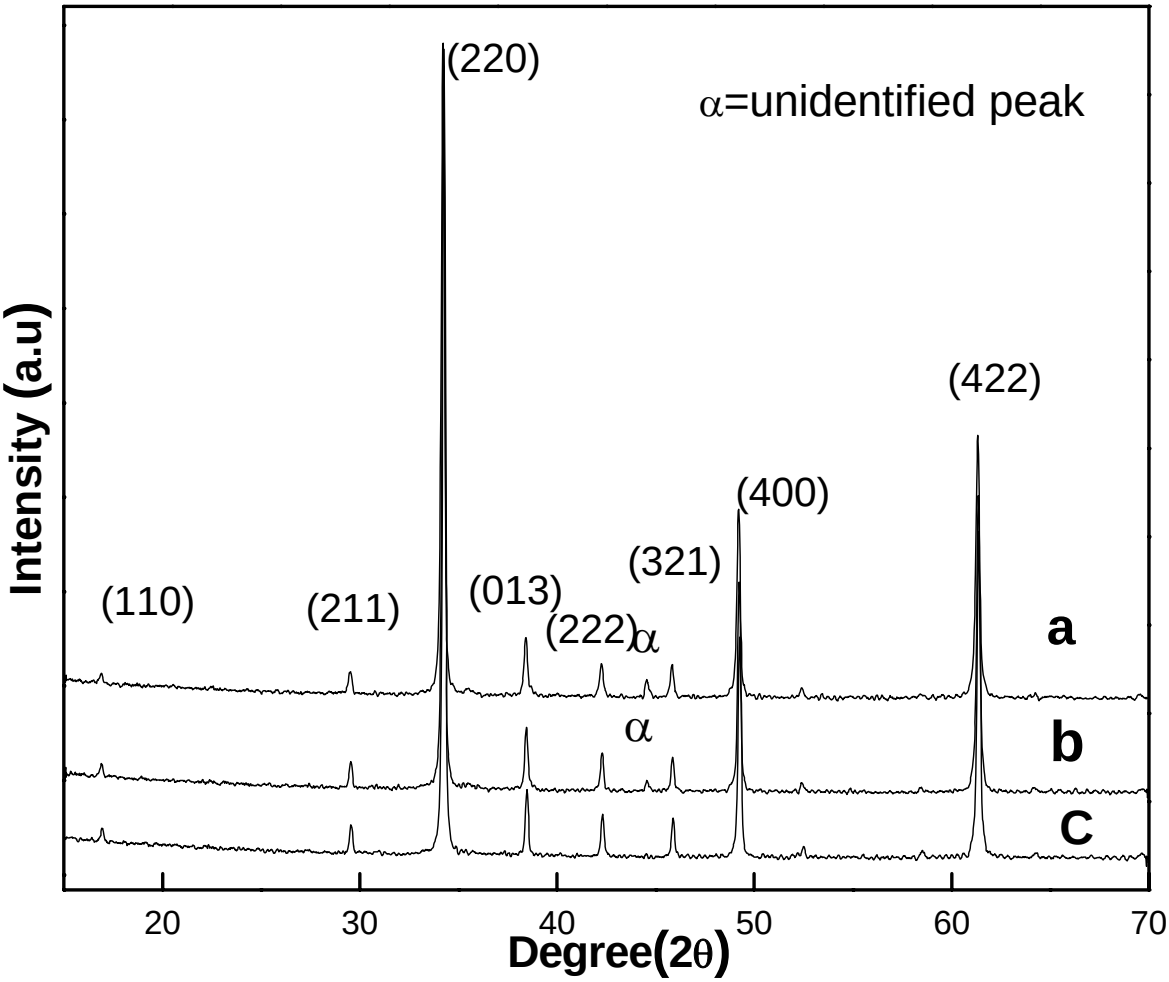

Fig 5.2.2 XRD patterns of $CaCu_3Ti_4O_{12}$ calcined at (a) 700°C, (b) 750°C, (c) 800°C

5.2.3 Particle size distribution of calcined $CaCu_3Ti_4O_{12}$ powder

The particle sizes distribution of the 800°C calcined powder is shown in Fig 5.2.3. It shows a monomodal particle distribution with particle size range in between 189-300 nm. The distribution shows that the distribution is narrow and has a width of only 110nm. It also confirmed from the X-ray that the particles are in the naometer range.

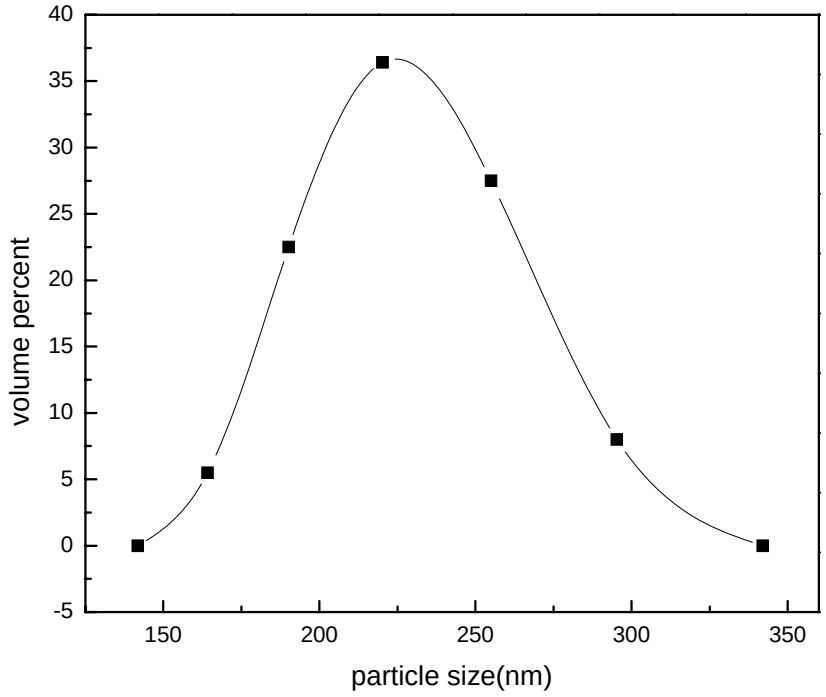

Fig 5.2.3 Particle size distribution curve of calcined $CaCu_3Ti_4O_{12}$ powder

5.2.4 Morhology of calcined CaCu3Ti4O12 powder

The morphology of the $CaCu_3Ti_4O_{12}$ powder calcined at 800^oC is shown in Fig. 5.2.4 as observed by SEM study. The distribution of the particles is shown in Fig. 5.2.4(a). This clearly indicated the particels are aggomerated and contsists of mostly large agglomerates with a very few small size particels in it. The magnified SEM micrograph of a agglomerate is shown in Fig.5.2.4 (b and c). It could be clearly observed that the agglomerates are actually formed from very samll particle in submicron range size. Althogh the agglomerates are of irregular size.

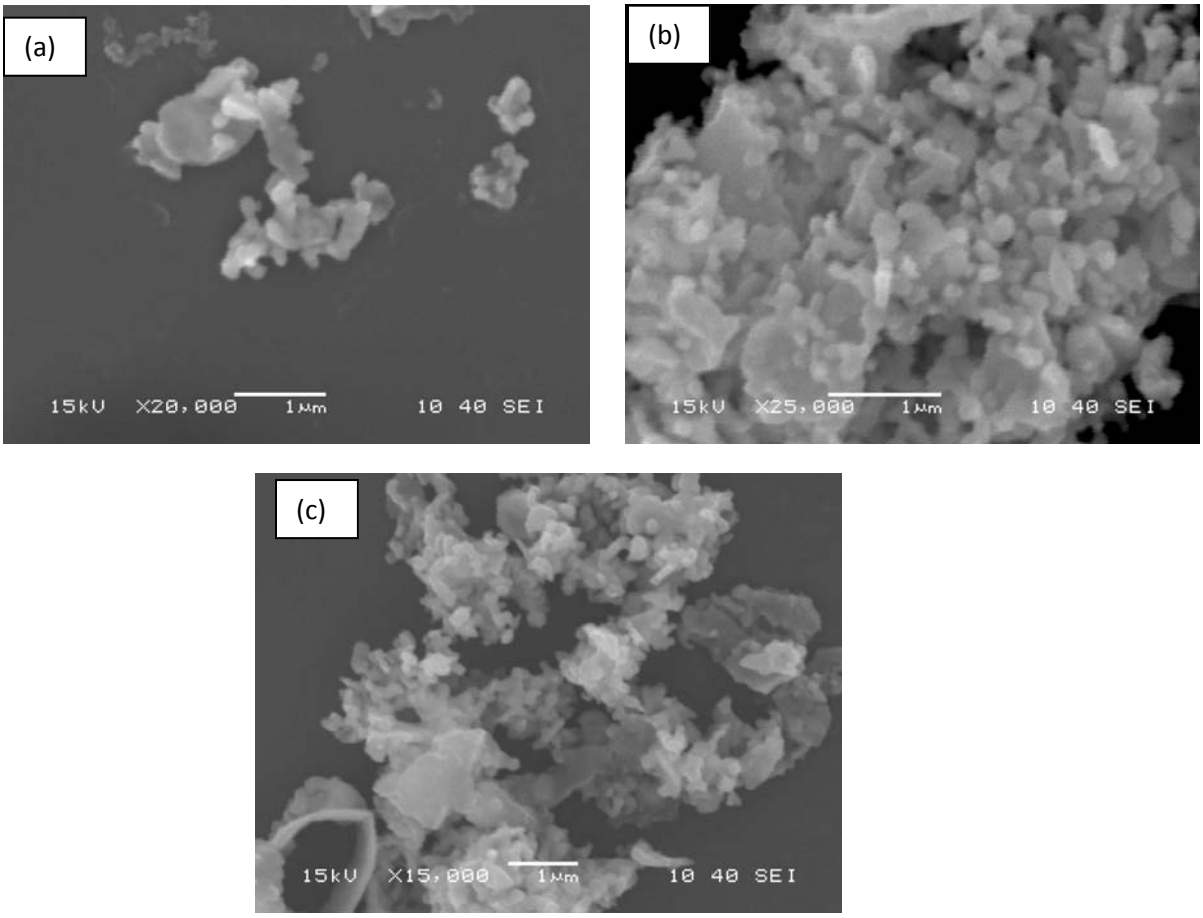

Fig. 5.2.4 SEM of $CaCu_3Ti_4O_{12}$ powder calcined at 800^oC

5.2.5 Phase analysis of sintered CCTO

The X-ray diffraction pattern of 1000^oC sintered pure CCTO samples have been provide in Fig.5.2.5 as a function of soaking time. Although no extra peak could be detected in the X-ray diffraction pattern of the samples sintered at 1000^oC/4hr, the X-ray diffraction pattern of the samples soaked for 6 hr contains some extra peak. This extra peak has been identified as TiO_2 phase. The formation of TiO_2 phase may be due to the formation some copper-calcium enriched grain boundary phases when the samples were sintered for a longer soaking time.

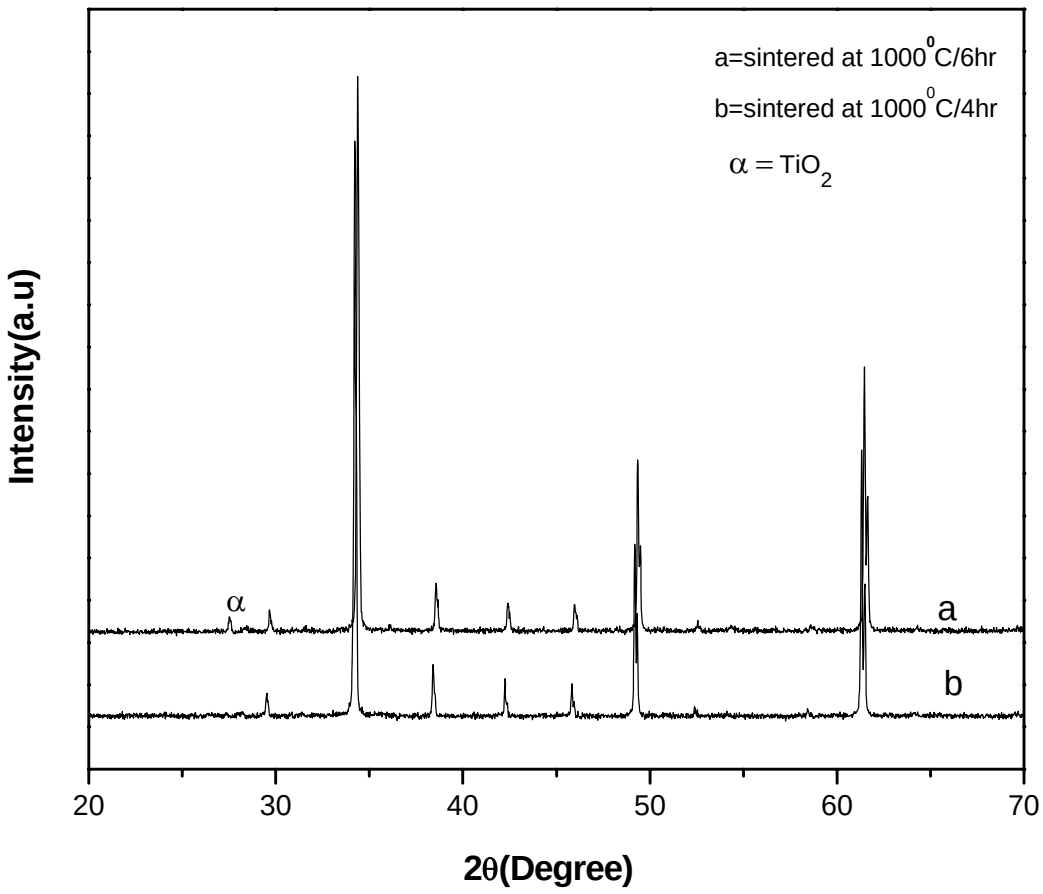

Fig 5.2.5 XRD pattern of $CaCu_3Ti_4O_{12}$ sintered at 1000^{0}C for 4hr and 6hr.

5.3 Sintering Behaviour of $CaCu_3Ti_4O_{12}$ Powder

Figure 5.3 represents the variation in shrinkage of the $CaCu_3Ti_4O_{12}$ samples as a function of sintering temperature. It could be seen from the figure that the samples undergoes a small expansion in the temperature range room temperature to 840^{o}C. This is quite natural and is due to the thermal expansion of $CaCu_3Ti_4O_{12}$ powder. The densification shrinkage was found to occur around 840^{o}C. The onset of the shrinkage may be due to the sintering of the material. The rate of shrinkage increases with temp and max at 980^{0}C after that decreases .The final shrinkage was 7% at 1000^{o}C.

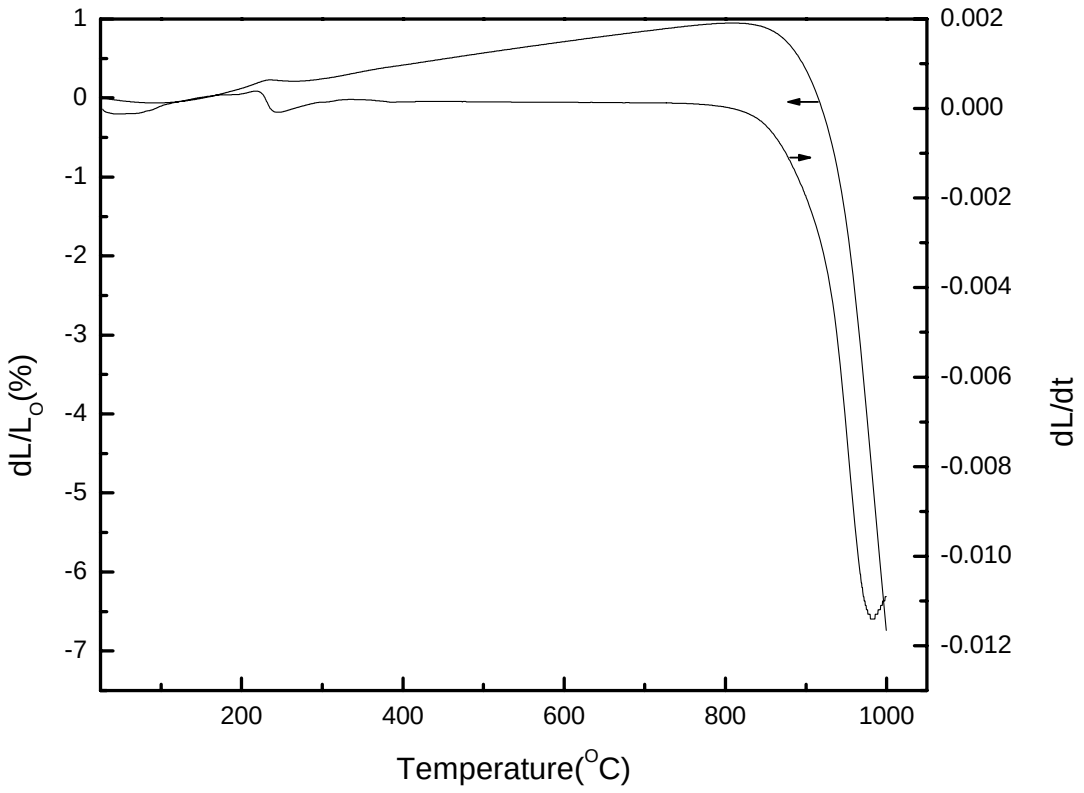

Fig. 5.3 Shrinkage behavior of $CaCu_3Ti_4O_{12}$ as a function of temperature.

5.4 Microstructure of Sintered $CaCu_3Ti_4O_{12}$ Ceramics

The SEM micrographs of the polished section of $CaCu_3Ti_4O_{12}$ samples sintered at 1000^{o}C for 4 hr and for 6hr have been shown in Fig. 5.4.(a,b) and (c,d) respecively. Submicron monomodal grain size distribution observed in the powder samples sintered at 1000^{o}C/4hr. Microstructure of the samples sintered at 1000^{o}C for 6 hr showed a matrix consisting of large grains wherein the small grains were embedded between the larger grains. The porosity present in the samples are intergranular in nature, the intragranular pores are not observed in both the cases. The grains are found to be regular and polyhedral types. The sample sintered at 1000^{o}C/6hr seems to be more denser in comparision with that sintered at 1000^{o}C/4hr. The densities of as-sintered samples were calculated by using Archimedes principle .The density was found to be 92.4% and 93.6% for samples sintered at 1000^{o}C for 4 hr and for 6 hr respectively.The grains size was found to increase with increasing in soaking time.

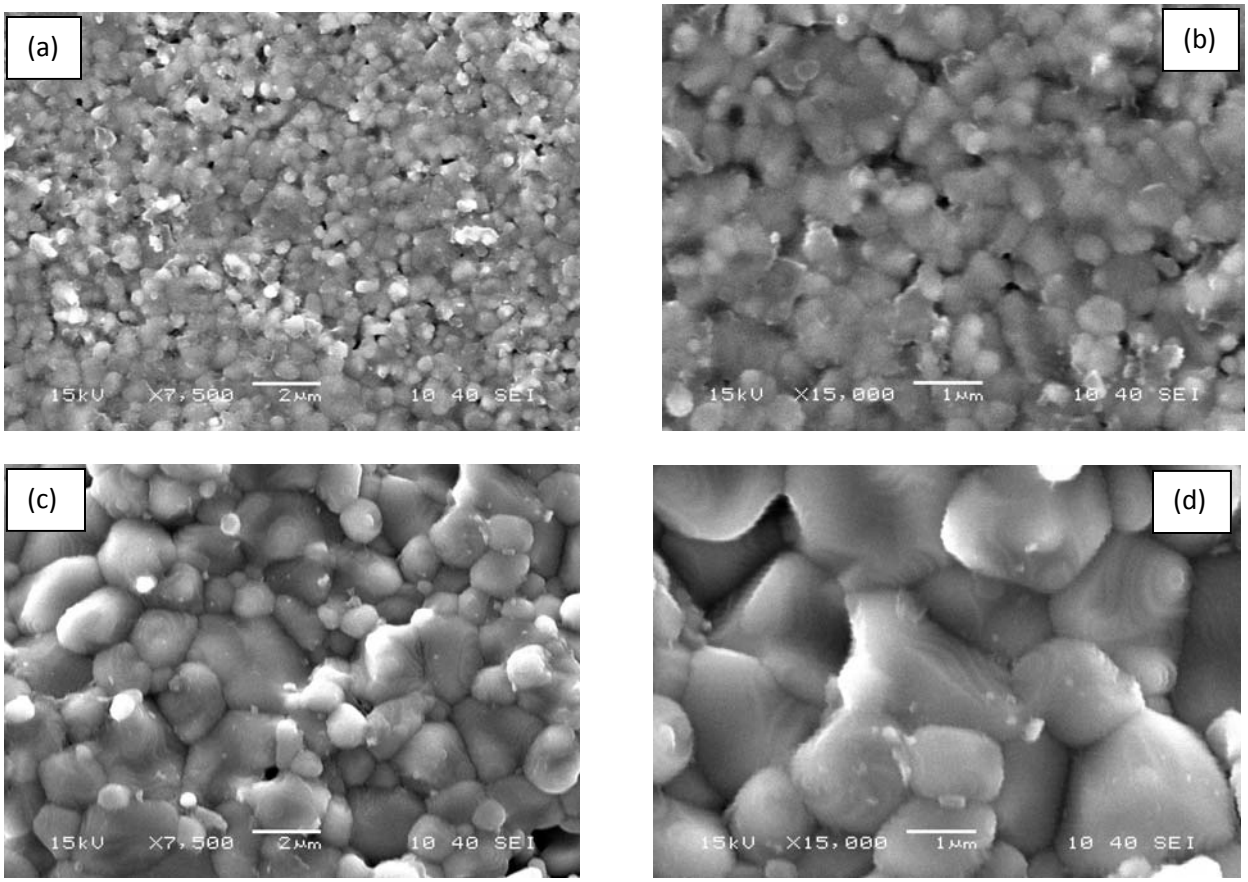

Fig. 5.4. SEM micrographs of sintered $CaCu_3Ti_4O_{12}$ samples (a and b) sintered 800°C/4hr, (c and d) sintered at 800°C/6hr.

5.5 Dielectric behaviour of $CaCu_3Ti_4O_{12}$

5.5.1 Room temperature dielectric behaviour of $CaCu_3Ti_4O_{12}$

The frequency dependent room temperature dielectric constant of the $CaCu_3Ti_4O_{12}$ samples has been presented in Fig. 5.5.1(a) as a function of soaking time sintered at 1000°C. The dielectric constant was found to increase with the soaking time. The increase dielectric constant may be correlated with porosity of the sample. The microstructural study revealed that the samples sintered at 1000°C/8hr have lower porosity than that sintered at 1000°C/4hr. The grain size of the samples sintered at 1000°C/8hr also high than that sintered at 1000°C/4hr. It could be found that the dielectric constant of the samples sintered at 1000°C for 8hrs is higher than 10^4 at frequency range from 10^2 to 10^5 Hz. The high dielectric constant suggests the

possibility that the charge carriers accumulate at the interface interaction of semiconducting grains and insulating grain boundary, which results in interfacial space charge polarization [79]. Li et al. [44] reported that the dielectric constant of polycrystalline CCTO at the high-frequency limit corresponds to that of grain volume, and at the low frequency limit is an apparent value which is the product of the dielectric constant of the grain boundary and the ratio of dimension of the grain to that of the grain boundary. The ‘‘giant’’ permittivity value for ceramics sintered for higher soaking time is, therefore, associated with the presence of either thin, reoxidized grain boundary regions on the outer surfaces of the large semiconducting grains or to a secondary phase at the grain boundaries [13], which has not been detected by XRD and SEM (Figs.5.2.5 and 5.4). Further work is needed to distinguish these possibilities. Specifically, the frequency dependent dielectric behavior has a Debey-like relaxation with a steep decrease in dielectric constant at the frequency where it displays a relaxation peak. The Debye-like relaxation can be explained by the Maxwell–Wagner relaxation at the interfaces between the grains and their boundaries. However in the present study the same could not be observed in the studied frequency range.

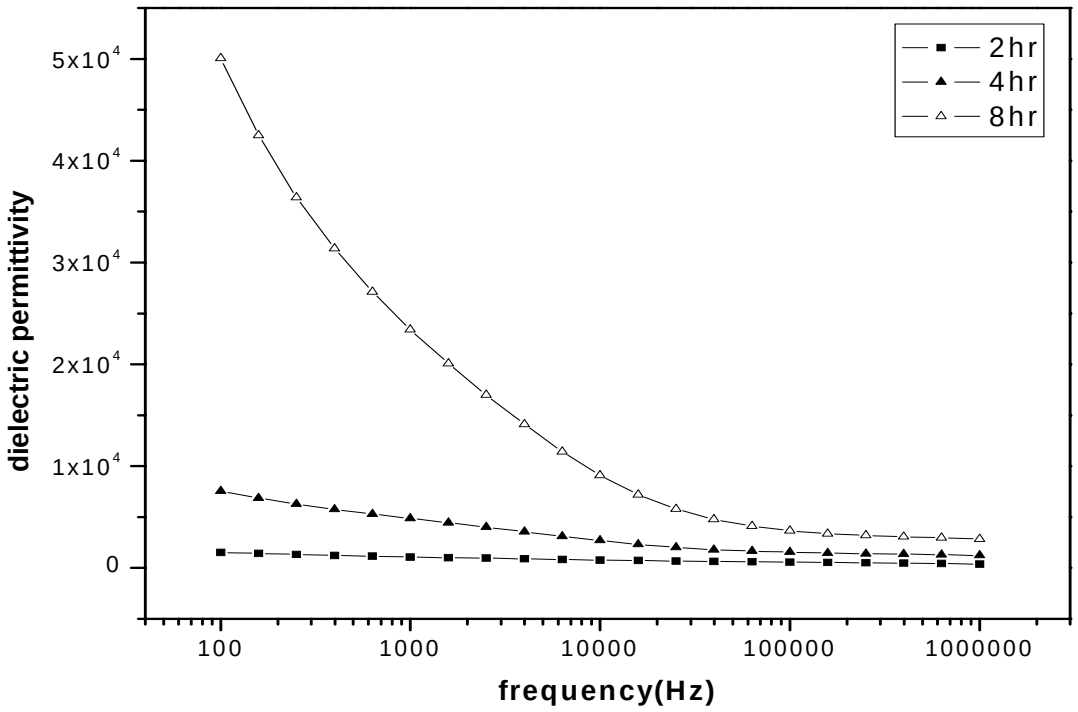

Fig. 5.5.1(a) Frequency dependent room temperature dielectric constant of $CaCu_3Ti_4O_{12}$ as a function of soaking time.

The frequency dependent dielectric loss (tanδ) of $CaCu_3Ti_4O_{12}$ is presented in Fig. 5.5.1(b) as a function of soaking time. The samples have been sintered at 1000°C. It could also be observed that there is no constant variation of tanδ value with frequency. The dielectric loss of the samples increases with increase in soaking time in the low frequency range (lower than 10^5 Hz). Longer sintering time will produce more oxygen vacancies and space charges, thus, more obvious dielectric relaxation can be observed giving rise to more dielectric losses [45].

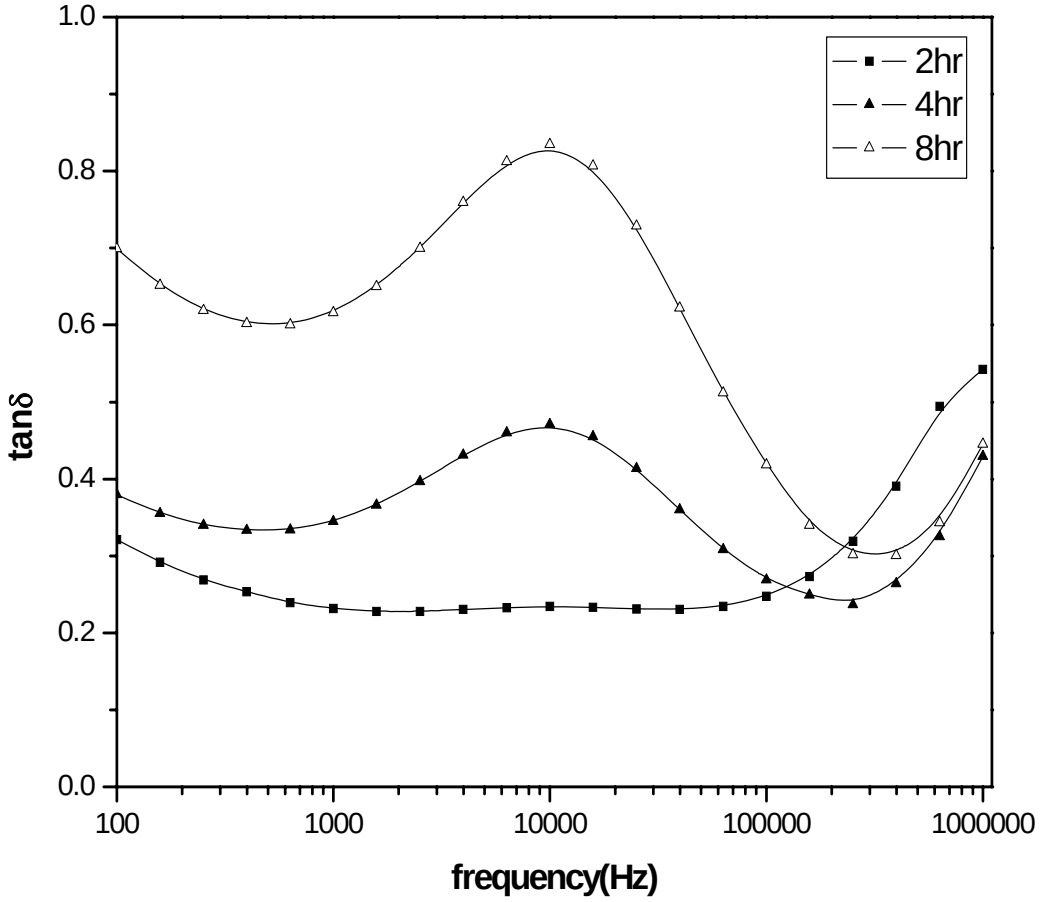

Fig.5.5.1 (b) Room temperature frequency dependence dissipation factor (tanδ) of $CaCu_3Ti_4O_{12}$ as a function of soaking time.

5.5.2 Temperature dependent dielectric behaviour of $CaCu_3Ti_4O_{12}$

The temperature dependent dielectric constant and dissipation factor (tanδ) of pure CCTO samples sintered at 1000°C/4hr is given in Fig. 5.5.2 (a-b). Wherein Fig. 5.5.2 (a) shows the temperature dependence dielectric constant and Fig. 5.5.2 (b) shows the variation of

dissipation factor. It has been observed that the relative permittivity increases with increase in temperature and decreases with increase in frequency. The lower dielectric constant observed at higher frequency is obvious and resulted from the dielectric relaxation [45]. The dielectric loss was also found to increase with increase in temperature. The dissipation factor (tan δ) for sample was found low in the entire temperature range studied (Fig. 5.5.2(b)) at high frequency. However, the same was found to increase rapidly above 140^{o}C at low frequency.

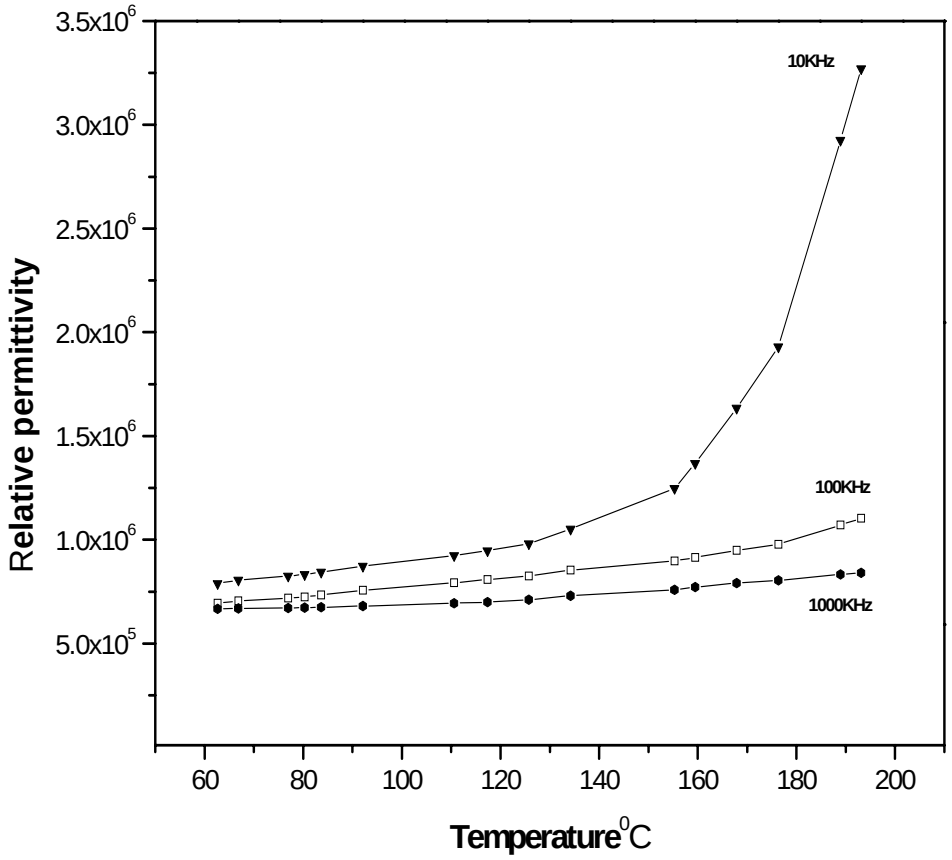

Fig.5.5.2 (a) Temperature dependent relative permittivity of $CaCu_3Ti_4O_{12}$ ceramics sintered at 800^{o}C/4hr.

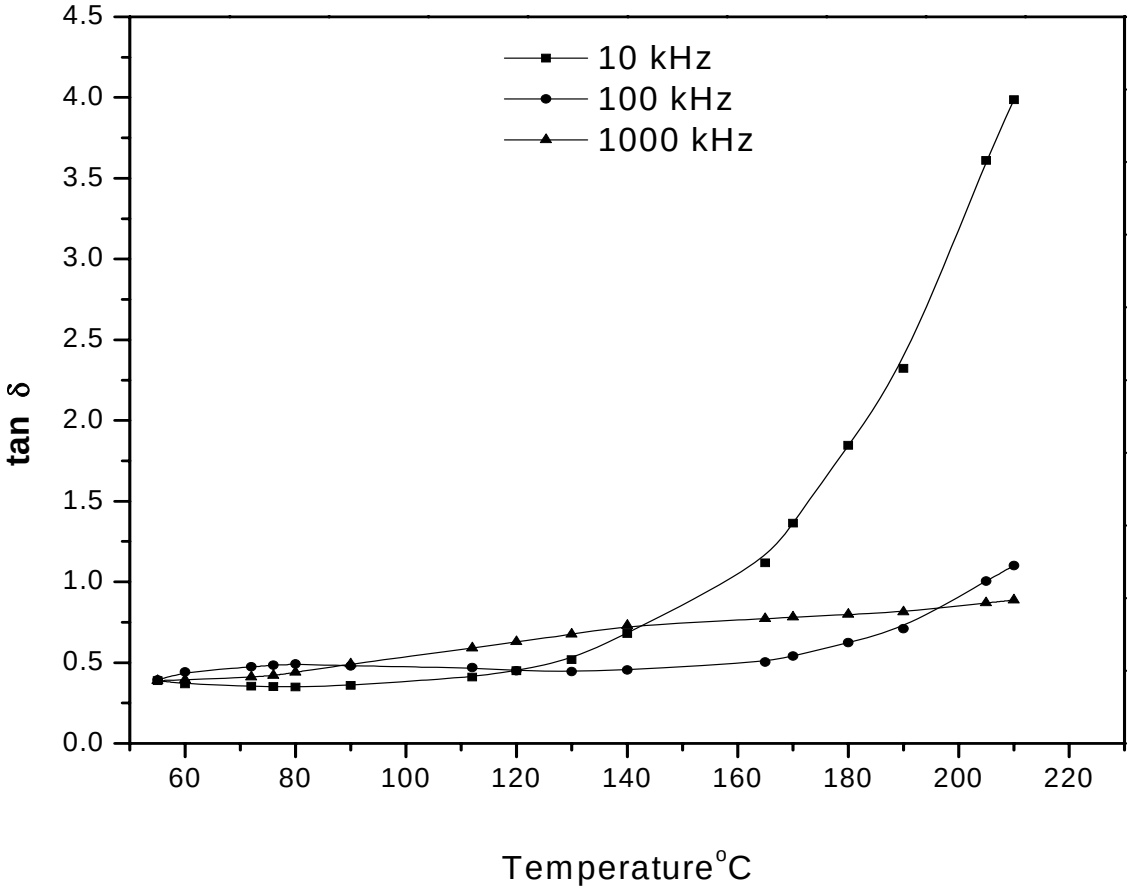

Fig.5.5.2 (b) Temperature dependent dissipation factor (tanδ) of $CaCu_3Ti_4O_{12}$ ceramics sintered at 800°C/4hr.

5.6 Synthesis of $Ca_{1-x}La_xCu_3Ti_4O_{12}$

Lanthanum doped CCTO ($Ca_{1-x}La_xCu_3Ti_4O_{12}$) where x= 0.02, 0.03, 0.04 and 0.05 mole have been synthesized following cobustion sythesis technique as discussed earlier. The phase evolution of the powder, microstructure development and dielectric properties of as-sintred sample etc. have been discussed as follows.

5.6.1 X-ray diffraction pattern of calcined $Ca_{1-x}La_xCu_3Ti_4O_{12}$ powder

XRD patterns of $Ca_{1-x}La_xCu_3Ti_4O_{12}$ powder calcinated at 800^0C for 4 hour have been shown in Fig 5.6.1 as a function of lanthanum substitution. XRD patterns were similar to that of pure $CaCu_3Ti_4O_{12}$. There is no evidence of secondary phases. From XRD, it has also been observed that the (100) peak shifted towards smaller angle with La substitution up to 0.04 mole lanthanum. Thereby the lattice parameter increases with increase in La concentration indicating the La_2O_3 goes into the solid solution of CCTO.

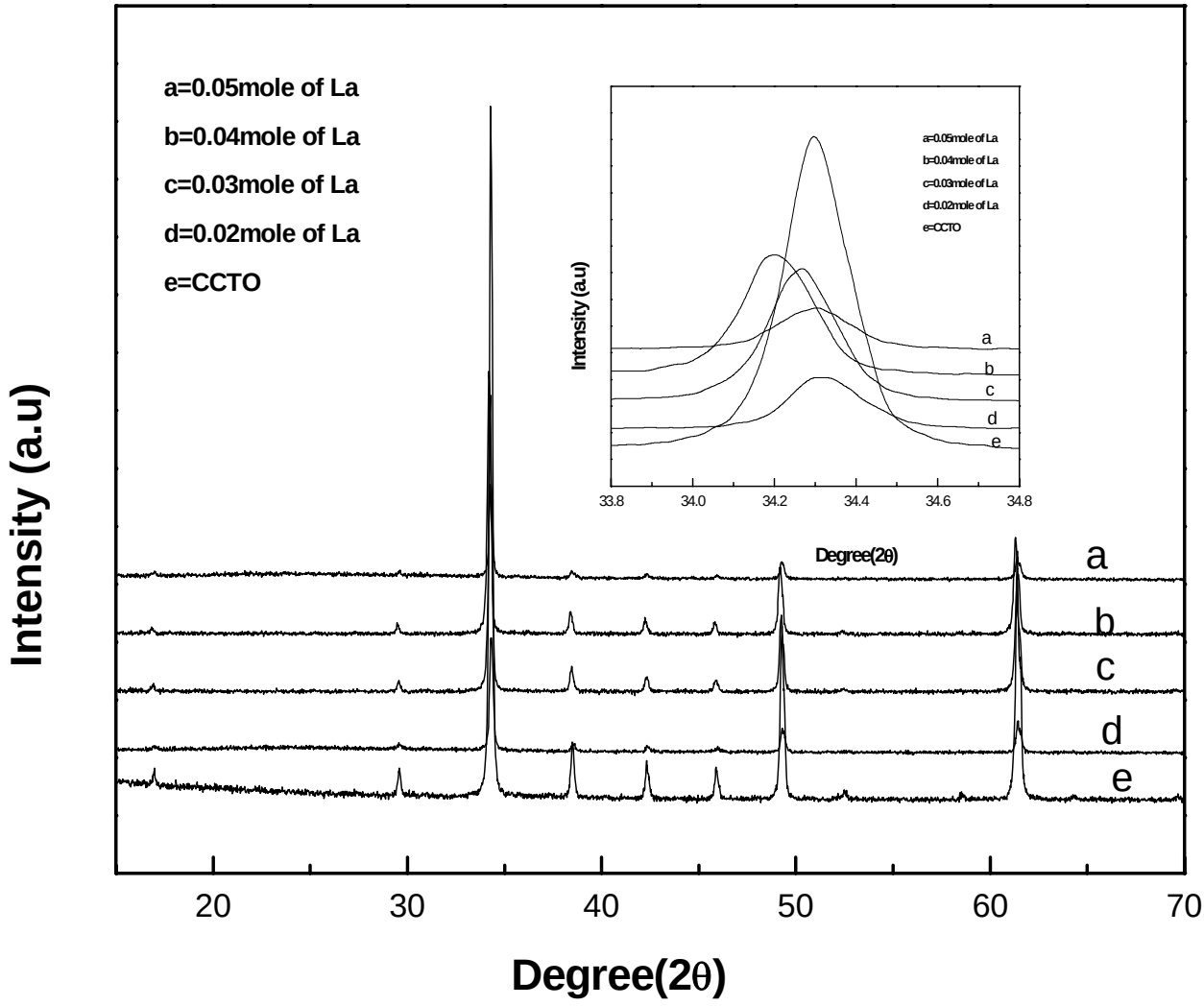

Fig.5.6.1 XRD for $Ca_{1-x}La_xCu_3Ti_4O_{12}$ ceramics with x=0.02, 0.03, 0.04 and 0.05

5.6.2 X-ray diffraction pattern of sintered $Ca_{1-x}La_xCu_3Ti_4O_{12}$ powder ceramics.

The X-ray diffraction pattern of the 1000^{o}C/4hr sintered samples has been presented in Fig.5.6.2 as a function of lanthanum doping. The major peaks of the X-ray diffractograms are identified to be that of CCTO. A small unidentified peak was observed in the both the X-ray pattern. The intensity of the unidentified peak was found to increase with lanthanum doping indicating that the amount of the phase increases with increase in lanthanum doping.

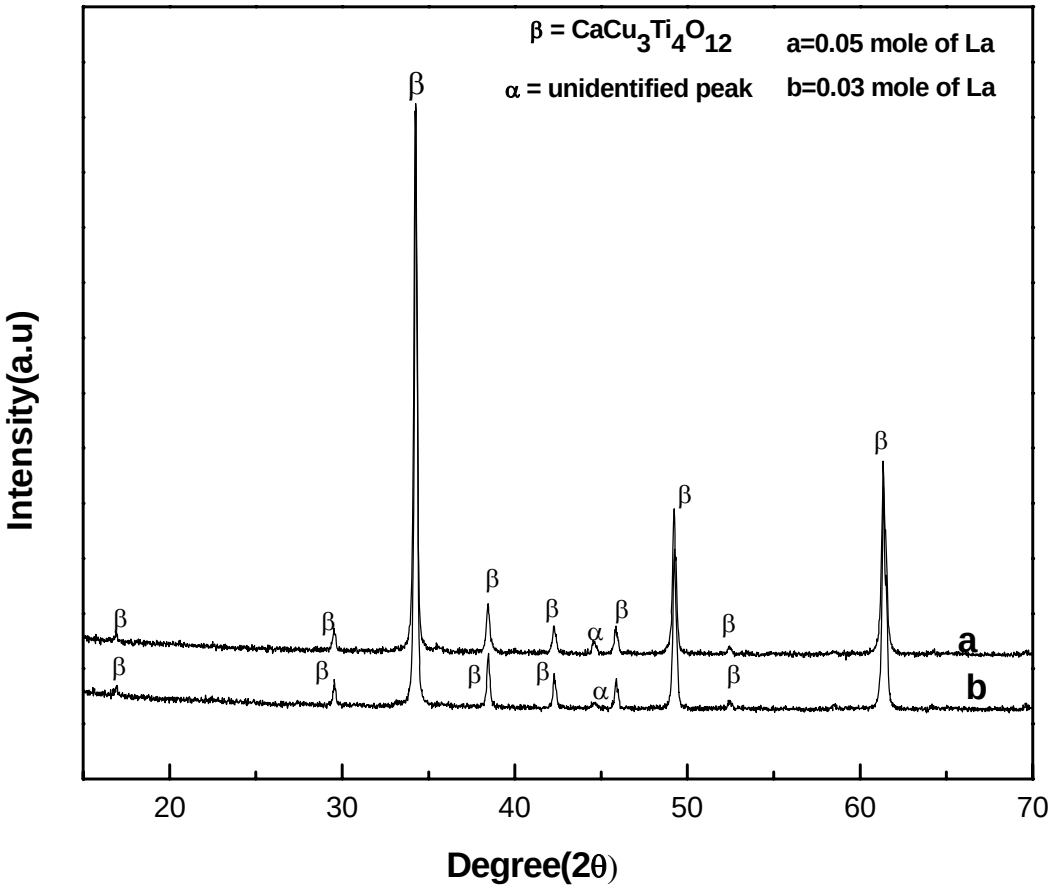

Fig.5.6.2 XRD for sintered $Ca_{1-x}La_xCu_3Ti_4O_{12}$ ceramics with x=0.03 and 0.05

5.6.3 Microstructure of sintered $Ca_{1-x}La_xCu_3Ti_4O_{12}$ ceramics.

SEM micrographs of 1000°C/4hrs sintered lanthanum doped CCTO ($Ca_{1-x}La_xCu_3Ti_4O_{12}$) samples (containing x=0.03, and 0.05 mole La_2O_3) has been presented in Fig.5.6.3. The average grain size was found to be larger in the samples containing 0.03 mole% La_2O_3 as compared to that containing 0.05 mole%. No secondary phase was indentified in the samples containing 0.03 mole% La_2O_3. However, the presence of a secondary phase has been clearly resolved in the micrographs of the samples containing 0.05 mole% La_2O_3. This secondary phase has been identified as a copper titanium enriched compound from the EDAX spectra. The presence of the secondary phase may be responsible for the grain refinement in the samples containing 0.05 mole% La_2O_3. The presence of an unidentified phase has also been detected in the X-ray diffraction spectra (Fig.5.6.3) of the sintered samples for both the cases, however the existence could not be resolved in the micrographs of the samples containing 0.03 mole% La_2O_3. This may

be due to the relatively small amount of the unidentified phase in the samples prepared with 0.03 mole% La_2O_3.

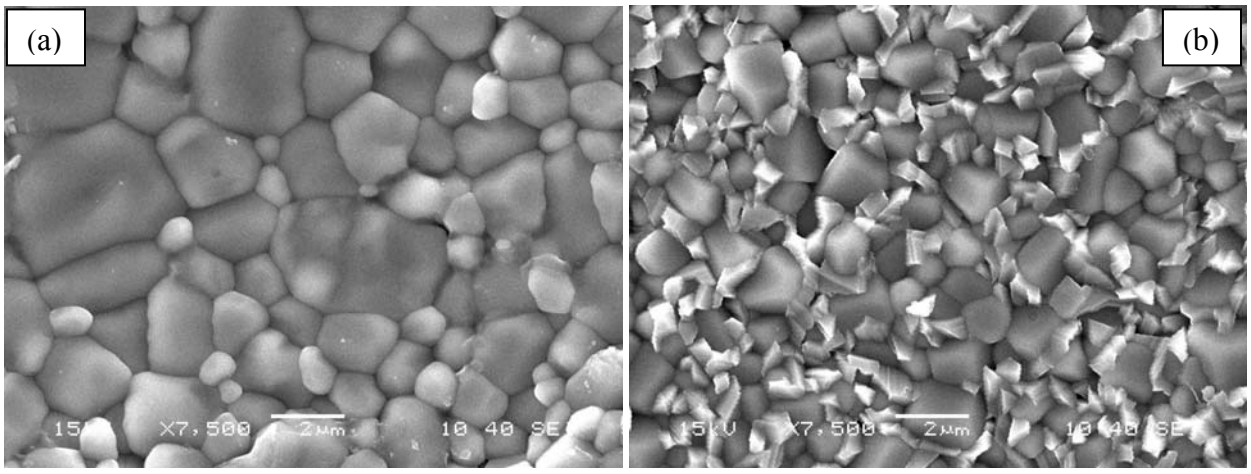

Fig. 5.6.3 SEM micrographs of sintered $Ca_{1-x}La_xCu_3Ti_4O_{12}$ samples (a) for x=0.03 (b)for x=0.05

5.7 Dielectric behaviour of $Ca_{1-x}La_xCu_3Ti_4O_{12}$

5.7.1 Room temperature dielectric behaviour of $Ca_{1-x}La_xCu_3Ti_4O_{12}$

The frequency dependence dielectric constant and dissipation factor (tan δ) of the samples prepared with 0.03 and 0.05 mole La_2O_3 is shown in Fig.5.7.1 (a) and (b) respectively. The dielectric constant and dissipation factor of pure CCTO has also been incorporated into the figure for comparison. The dielectric constant was found to increase with the increase in lanthanum doping. Although the dielectric dispersion was found more in the samples containing 0.03 mole% La_2O_3, it was almost negligible in the samples prepared with 0.05 mol% La_2O_3. The increase in dielectric constant with increase in lanthanum doping may be related to the formation of unknown copper titanium enriched grain boundary as observed by SEM micrographs and/or detected in the X-ray diffraction pattern. Dielectric dissipation was found to increase initially with the lanthanum doping and then it decreases. The dielectric dissipation was more in the samples prepared with 0.03 mole% La_2O_3 and was found to decrease with increase in frequency. The loss in the samples doped with 0.05 mol% La_2O_3 has a lower value than that containing 0.03 mol% La_2O_3.

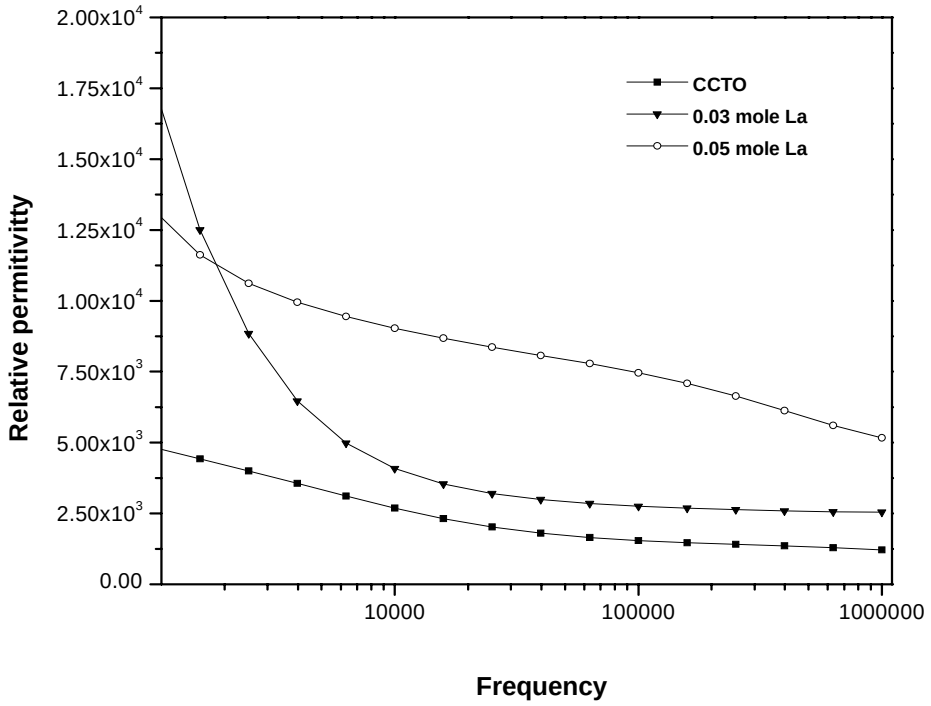

Fig. 5.7.1(a) Frequency dependent room temperature dielectric constant of pure $CaCu_3Ti_4O_{12}$ and $Ca_{1-x}La_xCu_3Ti_4O_{12}$ where x=0.03and 0.05.

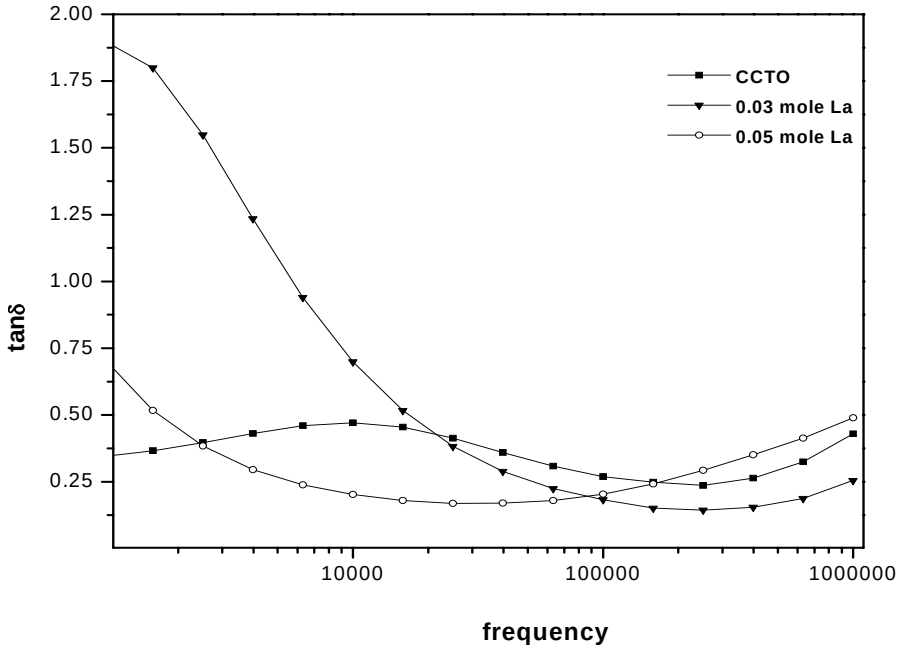

Fig. 5.7.1(b) Frequency dependent room temperature dissipation factor (tanδ) of pure $CaCu_3Ti_4O_{12}$ and $Ca_{1-x}La_xCu_3Ti_4O_{12}$ where x=0.03 and 0.05.

5.7.2 Temperature dependent dielectric behaviour of $Ca_{1-x}La_xCu_3Ti_4O_{12}$ (X=0.03)

The temperature dependent dielectric constant and dissipation factor (tanδ) of 0.03 mole% La_2O_3 doped CCTO samples sintered at 1000°C/4hr is given in Fig. 5.7.2 (a, b). Wherein Fig.5.7.2 (a) shows the temperature dependence dielectric constant and Fig.5.7.2 (b) shows the variation of dissipation factor. It has been observed that the relative permittivity increases with increase in temperature and decreases with increase in frequency. The lower dielectric constant observed at higher frequency is obvious and resulted from the dielectric relaxation [67]. The dielectric loss was also found to increase with increase in temperature. The dissipation factor (tan δ) for sample was found low in the entire temperature range studied (Fig.5.7.2 (b)) at high frequency. However, the same was found to increase rapidly above 160°C at low frequency.

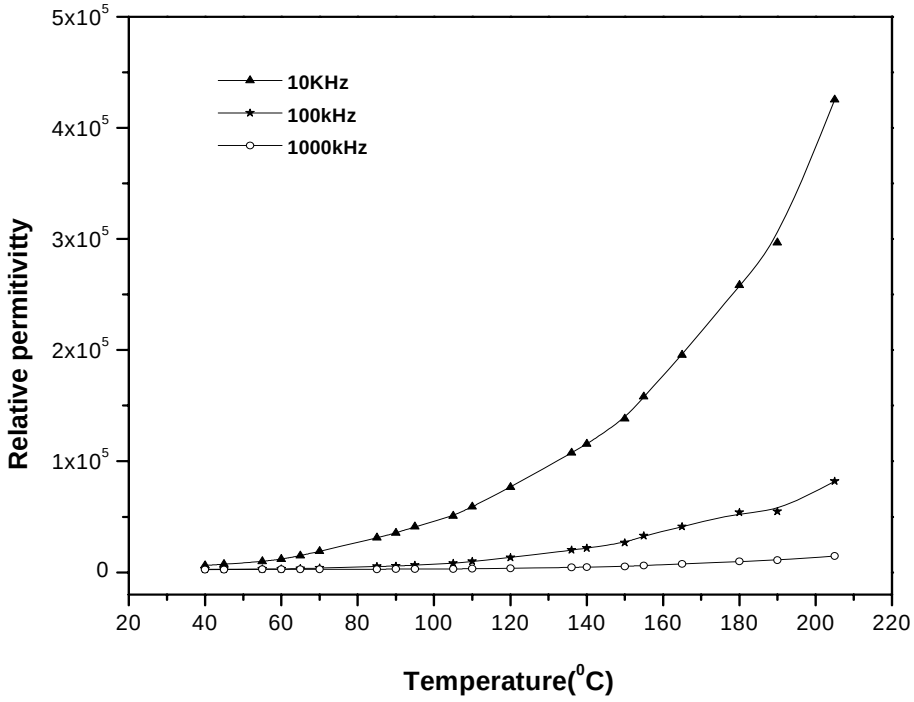

Fig. 5.7.2(a) Temperature dependent dielectric constant of $Ca_{1-x}La_xCu_3Ti_4O_{12}$ where x=0.03

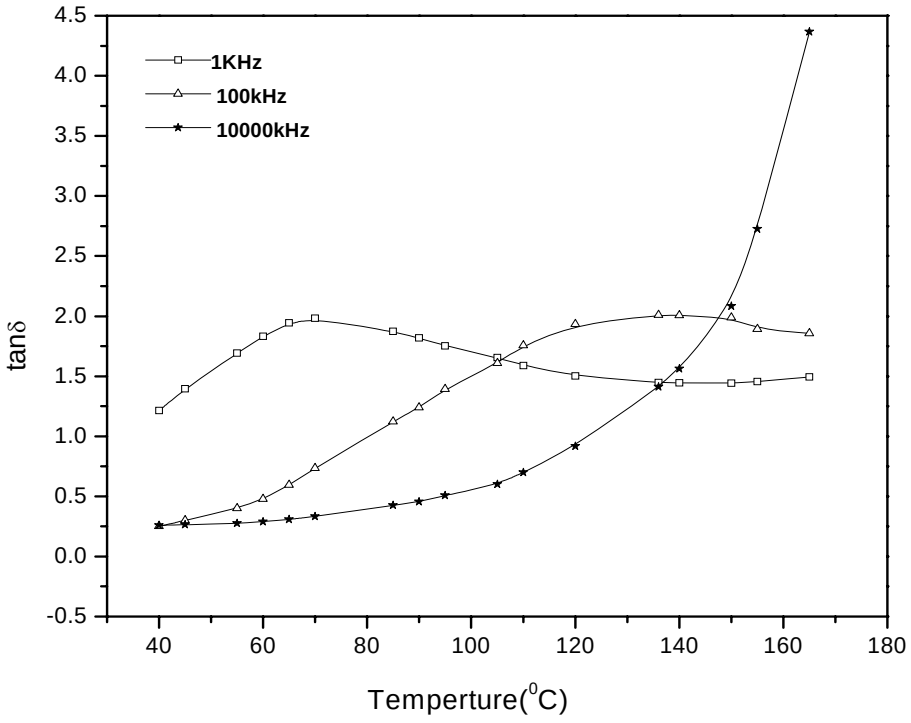

Fig. 5.7.2(b) Temperature dependent dissipation factor (tanδ) of $Ca_{1-x}La_xCu_3Ti_4O_{12}$ where x=0.03

5.7.3 Temperature dependent dielectric behaviour of $Ca_{1-x}La_xCu_3Ti_4O_{12}$ (X=0.05)

The temperature dependent dielectric constant and dissipation factor (tanδ) of 0.05 mole% La_2O_3 doped CCTO samples sintered at 1000°C/4hr is given in Fig. 5.7.3 (a, b).Wherein Fig.5.7.3(a) shows the temperature dependence dielectric constant and Fig.5.7.3(b) shows the variation of dissipation factor. It has been observed that the relative permittivity increases with increase in temperature and decreases with increase in frequency. The lower dielectric constant observed at higher frequency is obvious and resulted from the dielectric relaxation [67].. The dielectric loss was also found to increase with increase in temperature. The dissipation factor (tan δ) for sample was found low in the entire temperature range studied (Fig.5.7.3(b)) at high frequency. However, the same was found to increase rapidly above 160°C at low frequency.

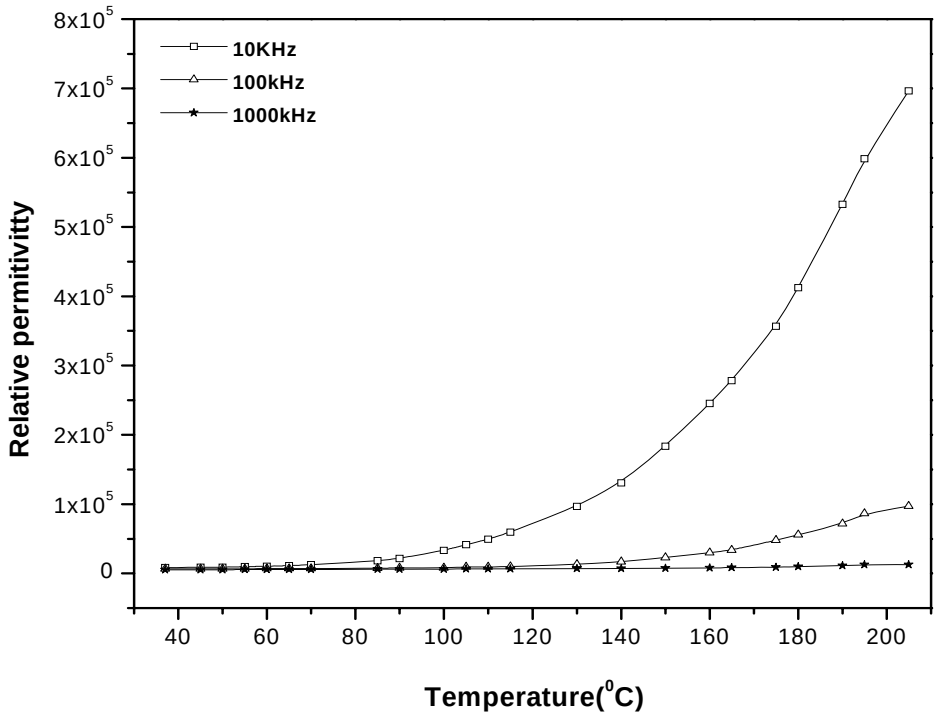

Fig. 5.7.3 (a) Temperature dependent dielectric constant of $Ca_{1-x}La_xCu_3Ti_4O_{12}$ where x=0.05

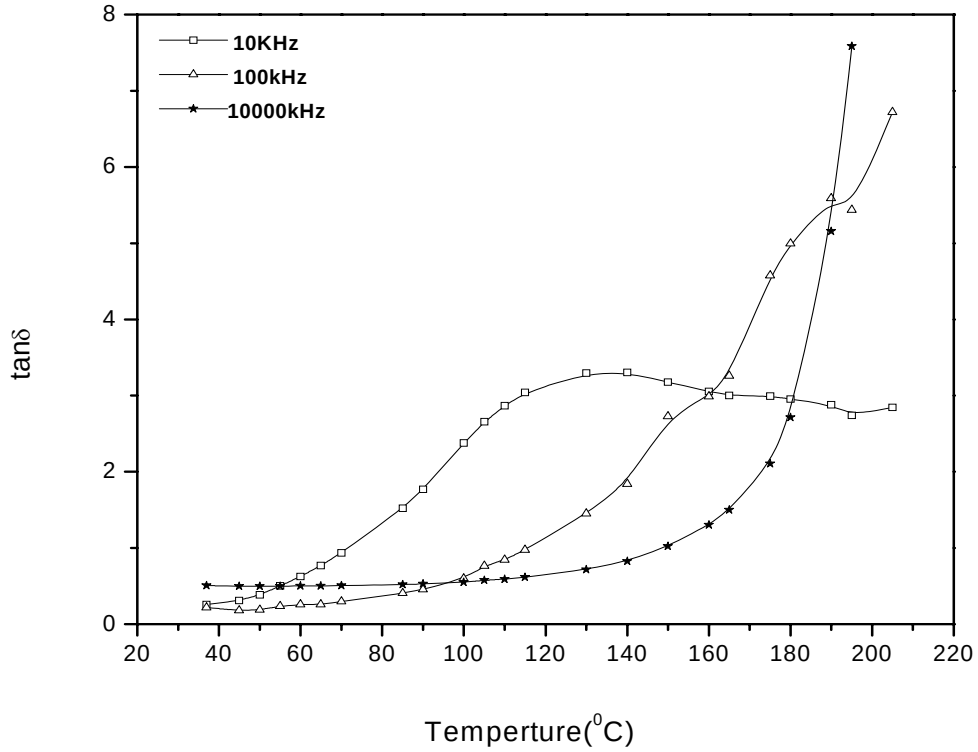

Fig. 5.7.3 (b) Temperature dependent dissipation factor (tanδ) of $Ca_{1-x}La_xCu_3Ti_4O_{12}$ where x=0.05

Chapter 6

CONCLUSION AND SCOPE OF FUTURE WORK

6.1. Conclusion

Phase pure $CaCu_3Ti_4O_{12}$ has been synthesized at lower temperature by modified citrate-nitrate auto-combustion process with optimized amount of citrate and nitrates. In order to get phase pure $CaCu_3Ti_4O_{12}$ at lower temperature the different process parameters citric acid, ammonium nitrate and pH had been optimized. The phase purity, powder morphology and the particle size distribution of the synthesized $CaCu_3Ti_4O_{12}$ powder and lanthanum doped $CaCu_3Ti_4O_{12}$ were also studied. The densification behavior, microstructure and dielectric behavior of the sintered specimens were studied. The following conclusions can be obtained from this study.

Citric acid content in the precursor solution should be kept 1.5 mole in order to achieve phase pure $CaCu_3Ti_4O_{12}$ at lower calcination temperature. The optimized amount of NH_4NO_3 was found to be 4 mole for the formation of phase pure CCTO. The pH also had a strong influence on the combustion synthesis of $CaCu_3Ti_4O_{12}$. The best results could be obtained at pH 1.The study revealed that for synthesis of $CaCu_3Ti_4O_{12}$ the precursor solution should have the composition $CaCO_3 : CuO : TiO(NO_3)_2 : C_6H_8O_7 : NH_4NO_3 = 1:3:4:1.5:4$.

X-Ray diffraction study revealed that phase pure $CaCu_3Ti_4O_{12}$ (CCTO) powders could be obtained on calcination at 800^0C/4hr. Average crystallite size calculated using Scherer's formula was found to be 66 nm when the powder calcined at 800^oC/4hr. Powder morphology study indicates that the powders are agglomerated. The agglomerates were of irregular shape.

From the microstructure study of sintered sample, it was found that the density was increased with increase in sintering time. The porosity present in the samples are intergranular in nature. The grains are found to be regular and polyhedral types.It was observed that the grains size was increased with increasing in soaking time.

Dielectric mesurement shows the dielectric constant increases with soaking time. It could also be observed that there is no constant variation of tanδ value with frequency. The dielectric loss of the samples increases with increase in soaking time.

XRD study revealed that lanthanum doping in CCTO, results and increase in the lattice parameters of CCTO indicating the La_2O_3 goes into the solid solution of CCTO. So it will affect the dielectric behaviour of the CCTO.

From SEM of as-sintered samples shows the average grain size is larger in the samples containing 0.03 mole% La_2O_3 as compared to that containing 0.05 mole%. A secondary phase has been identified from the EDAX spectra which may be responsible for the grain refinement in the samples containing 0.05 mole% La_2O_3.

It was observed from dielectric measurement that the dielectric constant was found to increase with the increase in lanthanum doping and dielectric dissipation was found to increase initially with the lanthanum doping and then it decreases.

6.2. Scope of Future Work

Optimization of different process parameters should be studied in detail from the study of the thermal decomposition behavior of the gel, surface area and particle size measurement, phase purity study.

Optimization of sintering schedule in order to achieve enhance densification of the sintered $CaCu_3Ti_4O_{12}$.and lanthanum doped $CaCu_3Ti_4O_{12}$ .Study of the densification and grain growth behavior during intermediate and final stageof sintering.

Study of the effect of lanthanum substituent on microstructure development and dielectric behaviour of $CaCu_3Ti_4O_{12}$.

Optimization of lanthanum substituent on the phase pure $CaCu_3Ti_4O_{12}$.

REFERENCE

[1]. Subramanian, M.A., Dong, L., Resiner, B.A., Sleight, A.W., 2000. High dielectric constant in $ACu_3Ti_4O_{12}$ phases. J. Solid State Chem. 151, 323–325.

[2]. Ramirez, A.P., Subramanian, M.A., Garbel, M., Blumberg, G., Li, D., Vogt, T., Shapiro, S.M., 2000. Giant dielectric constant response in copper-titanate. Solid State Commun. 115, 217–222.

[3]. Hongtao Yu, Hanxing Liu?, Dabing Luo, Minghe Cao,
journal of materials processing technology x x x (2 0 0 8) xxx-xxx

[4]. S. Ezhilvalavan, T.Y. Tseng, Mater. Chem. Phys. 65 (2000) 227.

[5]. L.C. Kretly, A.F.L. Almeida, R.S. de Oliveira, J.M. Sasaki, A.S.B. Sombra, Microw. Opt. Technol. Lett. 39 (2003) 145.

[6]. L.C. Kretly, A.F. Almeida, P.B.A. Fechine, R.S. de Oliveira, A.S.B. Sombra, J. Mater. Sci. Mater. Electron. 16 (2004) 657.

[7]. K. Thomas Jacob , Chander Shekhar , Xiaogan Li, Girish M. Kale
Acta Materialia 56 (2008) 4798–4803

[8]. Fang TT, Mei LT, Ho HF. Acta Mat 2006; 54:2867.

[9]. Shao SF, Zhang JL, Zheng P, Wang CL. Solid State Commun 2007;142:281.

[10]. J. Liu, Y. Sui, C. Duan, W.N. Mei, R.W. Smith, J.R. Hardy, Chem. Mater. 18 (2006) 3878.

[11]. C.C. Homes, T. Vogt, S.M. Shapiro, S. Wakimoto, A.P. Ramirez, Science 293 (2001) 673.

[12]. D. C. Sinclair, T. A. Adams, F. D. Morrison, and A. R. West, Appl. Phys. Lett. **80**, 2153 (2002).

[13] T. B. Adams, D. C. Sinclair, and A. R. West, Adv. Mater. (Weinheim, Ger.) **18**, 1321 (2002).

[14]. M. H. Cohen, J. B. Neaton, L. He, and D. Vanderbilt, J. Appl. Phys. **94**, 3299 (2003).

[15]. Lunkenheimer, R. Fichtl, S. G. Ebbinghaus, and A. Loidl, Phys. Rev. B **70**, 172102 (2004).

[16]. J. Liu, C. Duan, W.G. Yin, W.N. Mei, R.W. Smith, J.R. Hardy, Large dielectric constant and Maxwell–Wagner relaxation in Bi2/3Cu3Ti4O12, Phys. Rev. B 70 (2004) 144106-1–144106-6.

[17] J. Liu, C. Duan, W.N. Mei, R.W. Smith, J.R. Hardy, Dielectric properties and Maxwell–Wagner relaxation of compounds ACu3Ti4O12 (A = Ca, $Bi_{2/3}$, $Y_{2/3}$, $La_{2/3}$), J. Appl. Phys. 98 (2005) 93703-1–93703-5.

[18]. P. Lunkenheimer, V. Bobnar, A.V. Pronin, A.I. Ritus, A.A. Volkov, A. Loidl, Origin of apparent colossal dielectric constants, Phys. Rev. B 66 (2002) 52105- 1–52105-4.

[19]. S.Y. Chung, Lattice distortion and polarization switching in calcium copper titanate, Appl. Phys. Lett. 87 (2005) 52901.

[20] T.T. Fang, C.P. Liu, Evidence of the internal domains for inducing the anomalously high dielectric constant of CaCu3Ti4O12, Chem. Mater. 17 (2005) 5167–5171.

[21] J. Li, K. Cho, N. Wu, A. Ignatiev, Correlation between dielectric properties and sintering temperatures of polycrystalline CaCu3Ti4O12, IEEE Trans. Dielectr. Electr. Insul. 11 (2004) 534–541

[22] L. Fang, M. Shen, Effects of postanneal conditions on the dielectric properties of CaCu3Ti4O12 thin films prepared on Pt/Ti/SiO2/Si substrates, J. Appl. Phys. 95 (2004) 6483–6485.

[23] Y. Zhu, J.C. Zheng, L. Wu, A.I. Frenkel, J. Hanson, P. Northrup, W. Ku, Nanoscale disorder in CaCu3Ti4O12: a new route to the enhanced dielectric response, Phys. Rev. Lett. 99 (2007) 037602-1–037602-4.

[24] L. Wu, Y. Zhu, S. Park, S. Shapiro, G. Shirane, J. Tafto, Defect structure of the high-dielectric-constant perovskite CaCu3Ti4O12, Phys. Rev. B 71 (2005) 014118-1–014118-7.

[25] A.J.Moulson and J.M.Herbert. Electroceramics: materials, properties and applications (2nd edition).Publication-John Wiley and sons Ltd.

[26] Chih-Ming Wanga,_, Kuo-Sheng Kaob, Shih-Yuan Linc, Ying-Chung Chenc, Shang-Chih Weng Journal of Physics and Chemistry of Solids 69 (2008) 608–610

[27] Jianjun Liu, Robert W. Smith, and Wai-Ning Mei *Chem. Mater.* 2007, *19*, 6020–6024

[28] Chivalrat Masingboon , Prasit Thongbai , Santi Maensiri , Teerapon Yamwong , Supapan Seraphin, Materials Chemistry and Physics 109 (2008) 262–270

[29] Hongtao Yu, Hanxing Liu, Dabing Luo, Minghe Cao journal of materials processing technology x x x (2 0 0 8) xxx–xxx

[30] Laijun Liu, Huiqing Fan , Pinyang Fang, Xiuli Chen, Materials Research Bulletin 43 (2008) 1800–1807

[31] B. Barbier , C. Combettes , S. Guillemet-Fritsch , T. Chartier , F. Rossignol , A. Rumeaud, T. Lebey , E. Dutarde, Journal of the European Ceramic Society xxx (2008) xxx–xxx

[32] S. F. Shao, J. L. Zhang,a_ P. Zheng, W. L. Zhong, and C. L. Wang, J. Applied Physics, **99**, 084106 (2006)

[33] Z. Surowiak, M.F. Kupriyanov, D. Czekaj, J. Eur. Ceram. Soc. 21 (2001) 1377.

[34] H.Q. Fan, H.E. Kim, Japan., J. Appl. Phys. 41 (2002) 6768

[35] P. Thomas, K. Dwarakanath, K.B.R. Varma, T.R.N. Kutty, Journal of Physics and Chemistry of Solids 69 (2008) 2594– 2604

[36].Julie J. Mohamed, Sabar D. Hutagalung , M. Fadzil Ain , Karim Deraman , Zainal A.Ahmad, Materials Letters 61 (2007) 1835–1838

[37]. Kuznetsov, M. V., Parkin, I. P., Caruana, D. J. and Morozov, Y. G., *J. Mater. Chem.*, 2004, **14**, 1377–1382.

[38]. Patil, C. K., Aruna, S. T. and Mimani, T., *Solid State Mater. Sci.*, 2002, **6**, 507–512.

[39] . Berger, D. and Matei, C, *Rev. Roum. Chim.*, 2005, **50**, 889–894.

[40]. Deshpande, K., Mukasyan, A. S. and Varma, A., *J. Am. Ceram. Soc.*, 2003, **86**, 1149–1154.

[41]. J.S. Lian, X.Y. Zhang, H.P. Zhang, Z.H. Jiang, J. Zhang, Materials Letters 58 (2004) 1183–1188

[42]. S. Deka, P.A. Joy, Materials Chemistry and Physics 100 (2006) 98–101

[43] Jha, P., Arora, P., Ganguli, A.K. *Materials Letters*, 57 (2003) 2443-2446.

[44] J. Li, K. Cho, N. Wu, A. Ignatiev, IEEE Trans. Dielectr. Electr. Insul. 11 (2004) 534.

[45]. B.A. Bender∗, M.-J. Pan, Materials Science and Engineering B 117 (2005) 339–347

[46]. C.-F. Yang, Jpn. J. Appl. Phys. 35 (1996) 1806–1813.

[47]. C.-F. Yang, Jpn. J. Appl. Phys. 36 (1997) 188–193.

[48]. L. He, J.B. Neaton, M.H. Cohen, D. Vanderbilt, Phys. Rev. 65 (2002) 214112-1-11.

[49]. Seunghwa Kwona, Chien-Chih Huanga, M.A. Subramanianb, David P. Canna, Journal of Alloys and Compounds xxx (2008) xxx–xxx

[50]. T.B. Adams, D.C. Sinclair, A.R.West, J. Am. Ceram. Soc. 89 (9) (2006) 2833.

[51]. Kang-Min Kim, Jong-Heun Lee, Kyung-Min Lee, Doh-Yeon Kim, Doh-Hyung Riu, Sung Bo Lee, Materials Research Bulletin 43 (2008) 284–291

[52]. S.B. Lee, N.M. Hwang, D.N. Yoon, M.F. Henry, Metal. Mater. Trans. A 31A (2000) 985.

[53] . S.B. Lee, D.N. Yoon, M.F. Henry, Acta Mater. 48 (2000) 3071.

[54]. B.-K. Lee, S.-Y. Chung, S.-J.L. Kang, Acta Mater. 48 (2000) 1575.

[55]. S.-H. Lee, D.-Y. Kim, N.-M. Hwang, J. Eur. Ceram. Soc. 22 (2002) 317.

[56]. S.-H. Hong, D.-Y. Kim, J. Am. Ceram. Soc. 84 (2001) 1597.

[57]. M.-K. Kang, D.-Y. Kim, N.-M. Hwang, J. Eur. Ceram. Soc. 22 (2002) 603.

[58]. O.-S. Kwon, S.-H. Hong, J.-H. Lee, U.-J. Chung, D.-Y. Kim, N.-M. Hwang, Acta Mater. 50 (2002) 4865.

[59]. J.H. Ahn, J.-H. Lee, S.-H. Hong, N.-M. Hwang, D.-Y. Kim, J. Am. Ceram. Soc. 86 (2003) 1421.

[60]. Y.-S. Yoo, M.-K. Kang, J.-H. Han, H. Kim, D.-Y. Kim, J. Eur. Ceram. Soc. 17 (1997) 1725.

[61]. Jing Yang, Mingrong Shen, Liang Fang, Materials Letters 59 (2005) 3990 – 3993

[62]. J. Lia, A.W. Sleight, M.A. Subramanian, Solid State Communications 135 (2005) 260–262

[63]. D. Capsonia,b, M. Binia, V. Massarottia,b,_, G. Chiodellib, M.C. Mozzatica, C.B. Azzoni, Journal of Solid State Chemistry 177 (2004) 4494–4500

[64] . W. Kobayashi, I. Teresaki, Physica B 329–333 (2003) 771–772.

[65]. Shuhua Jin a,b, Haiping Xia a, Yuepin Zhang, Ceramics International 35 (2009) 309–313

[66].. A.F.L. Almeida, R.S. de Oliveira, J.C. Go´es, et al. Mater. Sci. Eng. B96(2002) 275–283

[67]. Alok KumarRai , K.D.Mandal , D.Kumar , OmParkash, Journal of Physics and Chemistry of Solids.

[68]. W. Kobayashi, I. Terasaki, Appl. Phys. Lett. 87 (2005) 032902–032904.

[69].S. F. Shao, J. L. Zhang,a_ P. Zheng, C. L. Wang, J. C. Li, and M. L. Zhao, Applied Physics Letters, **91**, 042905 (2007).

[70].L. X. Feng, X. M. Tang, Y. Y. Yan, X. Z. Chen, Z. K. Jiao, and G. H. Cao, Phys. Status Solidi A **203**, 22 (2006)

[71].D. Capsoni, M. Bini, V. Massarotti, G. Chiodelli, M. C. Mozzatic, and C. B. Azzoni,, J. Solid State Chem. **177**, 4494 (2004).

[72]. B. Shri Prakash and K. B. R. Varma, J. Mater. Sci.: Mater. Electron. **17**, 899 (2006

[73]. J. J. Liu, C. G. Duan, and W. N. Mei, J. Appl. Phys. **98**, 093703 (2005).

[74]. B. Shri Prakash and K. B. R. Varma, Physica B **382**, 312 (2006).

[75] Y. Y. Yan, L. Jin, L. X. Feng, and G. H. Cao, Mater. Sci. Eng., B **130**, 146 (2006).

[76] F. Deganello , G. Marcì , G. Deganello Citrate–nitrate auto-combustion synthesis of perovskite-type nanopowders: A systematic approach ,Journal of the European Ceramic Society 29 (2009) 439–450

[77] K.H. Wu, C.H. Yu, Y.C. Chang, D.N. Horng, Journal of Solid State Chemistry. Vol.177,pp.4119(2004)

[78] Tsang-Tse Fang and Jenq-Dar Tsay, J. Am. Ceram. Soc., 84 [11] 2475–78 (2001)

[79] H. Birey, J. Appl. Phys. 49 (1978) 2898

.